RSC Advances

ROYAL SOCIETY
OF CHEMISTRY

www.rsc.org/advances

RSC Advances

Transition Metal Complex Redox Shuttles for Dye-Sensitized Solar Cells

Babak Pashaei, Hahsem Shahroosvand* and Parisa Abbasi

Chemistry Department, University of Zanjan, Zanjan, IRAN.

Abstract:

An important link exists between the selected molecular structure of a sensitizer and the employed shuttle electrolyte to achieve high conversion efficiency in dye-sensitized solar cells (DSSCs). So far, the most commonly used redox mediator is iodide/triiodide (I^-/I_3^-), which has shown advantages such as desirable kinetic properties and high carrier collection efficiencies. However, it has several disadvantages including a low redox potential, corrosion toward metal materials and competitive blue light absorption. In this respect, the transition metal complex electrolytes represent valuable alternatives to replace with traditional I^-/I_3^- couples, which can overcome the drawbacks of I^-/I_3^- electrolyte. In recent years, the best efficiency of DSSC was achieved by porphyrin-sensitized solar cells with transition metal complex-based redox electrolyte. In particular, in 2014, the Gratzel group published a record DSSC efficiency of 13 % by using a new porphyrin sensitizer with Co-polypyridyl-based electrolyte. Here, we plan the engineering of structure of new transition metal complex electrolyte and the design of molecular structure of sensitizer in touch. The main focus will be held on the correlation between photophysical and electrochemical properties of the metal complex mediators and their DSSC performances. This review provides an in-depth investigation on the exciting alternative electrolyte shuttle in DSSCs and their various advantages that are endowed with both high conversion efficiency and non-corrosive properties.

1. Introduction

As a promising technology for the new generation of photovoltaic systems, dye-sensitized solar cells (DSSCs) have attracted tremendous attention due to their low manufacturing costs, environmentally acceptable energy, renewable and high power conversion efficiency.[1] The main components of a DSSC are a cathode, sensitizer dye, photoanode and an electrolyte solution containing a redox couple. The photoanode is a porous nanocrystalline semiconductor metal oxide such as TiO_2, ZnO layer coated with a monolayer of chemisorbed sensitizers, supported on a conductive glass substrate (SnO_2:F). The ideal sensitizer has to meet several requirements that guide effective molecular engineering: (i) a broad and strong absorption to absorb all incident lights below the near-IR wavelength; (ii) the presence of anchoring groups such as carboxylates or phosphonates to anchor on the surface of semiconductor; (iii) a sufficiently higher reduction potential for sensitizer LUMO (lowest unoccupied molecular orbital) than the semiconductor conduction band edge. This property minimizes the energetic potential losses during the electron transfer reaction and (vi) a sufficiently lower oxidation potential of sensitizer HOMO (highest occupied molecular orbital) than the redox potential of the electron mediator species to accept electron donation from an electrolyte or a hole conductive material, (v) 10^8 turnovers corresponding to 20 years exposure to sunlight without apparent degradation.[2] The cathode which usually consists of Pt coated SnO_2:F is separated from photoanode by a ~ 20 μm thick gasket made of a polymer. The redox electrolyte solution injects between the electrodes and penetrates the semiconductor layer pores, intimately contacting the dye monolayer.

In operation, the dye catches the photons from incoming light and uses its energy to excite the electrons, the same as chlorophyll in photosynthesis. The dye injects this excited electron into TiO_2 and the electron is conducted away by nanocrystalline semiconductor. The electrons can be transported into the semiconductor film as the

conducting electrons. In addition, the counter electrode (CE) collects the electron from the external circuit, and catalyzes the reduction of tri-iodide electrolyte ions (Fig. 1).[3-5]

As one of the most critical functional components in DSSCs, the redox electrolyte has been demonstrated to be very crucial in determining the photoelectric conversion efficiency and device stability of DSSCs.[6,7] So far, the most commonly used redox mediator is iodide/triiodide (I^-/I_3^-) couple, which showed the best-performing and efficient electrolyte in DSSCs owing to their high carrier collection efficiencies and desirable kinetic properties.[1]

However, the I^-/I_3^- redox couple suffers from these intrinsic disadvantages: (a) it is very corrosive towards metals such as Ag, Au and Cu. So the use of such materials as current collectors in DSSC modules which require long-term stability is excluded; (b) it absorbs the visible light, reducing the photocurrent and competitive light absorption and consequently the power efficiency; and (c) the formation of the intermediate radical species I in dye regeneration process, which exhibits a more negative redox potential than the corresponding standard redox potential of I^-/I_3^-. It represents an additional energy activation barrier for the dye regeneration. For example, DSSCs based on the benchmark sensitizers, such as N719 (di-tetrabutylammonium-cis-bis(isothiocyanato)bis(2,2′-bipyridyl-4,4′-dicarboxylato)ruthenium(II)), the difference between the redox potential of the dye, $E(D/D^+)$ (1.0–1.1 V), and the I^-/I_3^- redox couple, $E(I^-/I_3^-)$ (E^0 ranges from 0.35 V in acetonitrile to typically 0.4 V for electrolytes optimized for ruthenium sensitizer-based DSSCs), is in excess of 600 mV. For photons having an energy of 2 eV, this means that more than 30% of the original photon, which limits the open circuit voltage (V_{oc}) to 0.7–0.8 V. 200 mV driving force is enough for efficient dye regeneration, which implies a loss of 0.5 V open circuit voltage.[8,9]

In the area of iodine-free redox couples for DSSCs, attempts to find alternatives to the I^-/I_3^- redox shuttle have been limited to three series of redox couples which include transition metal-complexes, organic redox shuttles[10-16] and hole transporting materials[17-23]. However, one-electron outer sphere redox shuttles based on transition metal complexes have shown the most attention compared to the others.

Chemistry Department, University of Zanjan, Zanjan, IRAN.
E-mail: shahroos@znu.ac.ir
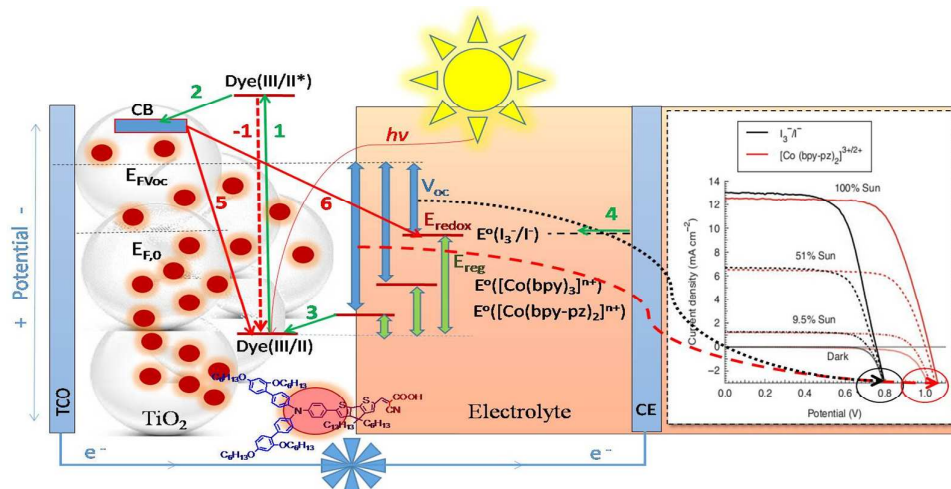
Fig. 1 Left: Operating principle of a nanocrystalline DSSCs. Schematic illustration of the electron-transfer processes occurring at the dye-sensitized heterojunction: process 1, photoexcitation of the sensitizing dye; process -1, decay of excited sensitizer; process 2, electron injection into the conduction band (CB) of the TiO_2 semiconductor; process 3, dye regeneration via accepting electrons from the reduced state of the redox couple and producing the oxidized state of the redox couple in electrolyte; process 4, dye regeneration via hole transporting medium; process 5, back electron transfer to the oxidized dye; process 6, the recombination process between the injected electron and the oxidized species in the hole transporting medium; The indirect path of the oxidized redox shuttle is depicted; however, the actual path is more complicated and much longer. The green arrows indicate the positive processes and the red arrow indicates the deleterious processes. Right: comparison of I–V curve for the Y123 dye with $[Co(bpy-pz)_2]^{2+/3+}$ (Table 3) (red lines) and I^-/I_3^- (black lines) electrolytes.[24]

Therefore, there is the requirement to optimize the cells and develop alternative electrolyte shuttles, to replace iodide with lower mismatch between the oxidation potential of the dye and the redox couple. In addition, these alternative redox couples should exhibit improved physical and chemical properties such as good solubility, high thermal stability, substantially optically clear at concentrations permitting good conductivity and finally noncorrosive toward the components of the solar cell. For this reason, the development of alternative redox mediators should further improve the technology of DSSCs.

In 2010, a breakthrough paper by Feldt et al. reported that a DSSC employing the transition metal complex as a redox shuttle, $[Co(bpy)_3]^{2+/3+}$ (bpy= 2,2'-bipyridine), could achieve an efficiency of 6.7% when combined with an organic dye.[25] However, a large volume of the recent works on DSSCs is devoted to the substitution of I^-/I_3^- redox couple with alternative material. Meanwhile, a great number of transition metal complexes especially Co, Cu and Ni polypyridyl complexes were reported to overcome the disadvantages of traditional I^-/I_3^-.[26] One of the advantages of metal polypyridyl based redox electrolytes is the lower absorption in the visible range compared to the triiodide species[24,27] and that they show no corrosive behavior towards metal contacts. This characteristic is important for durability of DSSC devices for commercial applications. Another attractive feature of metal complexes electrolytes such as cobalt polypyridyl complexes is the facile tuning of their redox potential by varying the ligands with different electron withdrawing or donating groups. Depending on the HOMO level of the dye, the redox potential of the metal complex electrolyte can be tuned to the required range in order to have sufficient driving force for the dye regeneration to enable maximum open circuit voltages.[9]

Furthermore, the ligand properties can be tuned to modulate the relative activation energies for electron-transfer processes in metal complexes.[28,29] Besides the Co(II/III) complexes as efficient redox mediators, several transition metal compounds were also proposed. $[VO(salen)]^{0/+}$ (salen= N,N'-ethylenebis(salicylideneiminate)(2−))[30], $[Ni(dicarbollide)_2]^{0/−1}$ [31] and ferrocene/ferrocenium (Fc/Fc^+)[32] are some of these complexes.

As seen in Fig. 2, this field is growing fast and there is an exponential growth in both publications and citations dealing with the role of complex electrolyte in DSSCs.

This review concentrates on employment of different metal complexes for engineering of new electrolyte in DSSCs. It also systematically introduces several approaches to design transition metal complex electrolytes based on different chelated ligands. It covers not only the most frequently reported complexes, but also describes some conventional organic dyes that led to promising results so far. Moreover, the review will survey an introduction to the exclusive position of organic and porphyrin dyes as optimized sensitizers, to present the interest of readers in this field. Therefore, the main idea is to inspire readers to explore new avenues in the design of novel transition metal complex electrolytes instead of I^-/I_3^- couple.

2. Co-based redox mediators
2.1 Co-bipyridine-based mediators

In 2002, Sapp and co-workers studied a series of cobalt complexes including terpyridine, bipyridine, and phenanthroline.[33] DSSCs based on $[Co(dtb)_3]^{2+/3+}$ (Table 1) and dye N3 electrolyte showed the best efficiency of 80% of that of a comparable I^-/I_3^--mediated DSSC. The electrochemical results indicated a dramatic surface dependence of the electron-transfer kinetics, which empirical evidence suggests is a necessary attribute for an efficient mediator. In the following, the same group improved characteristics of the $[Co(dtb)_3]^{2+/3+}$ as electrolyte, through adding a co-mediator (PZT= phenothiazine or ferrocene) with ability of quickly electron transfer.[34] The I-V curve outcomes showed that using PZT/Co(II) mixture as mediator leads to more desirable performance compared to Co(II/III)-based systems. Furthermore, both V_{oc} and FF in PZT/Co(II) cell remarkably increased with respect to I^-/I_3^--based cells. They also observed that PZT/Co(II) system is more efficient than Fc/Co(II) mixture system. Because the interception of Fc^+ by Co(II) is not fast enough to prevent recombination between Fe(II) and the electrons in the TiO_2.
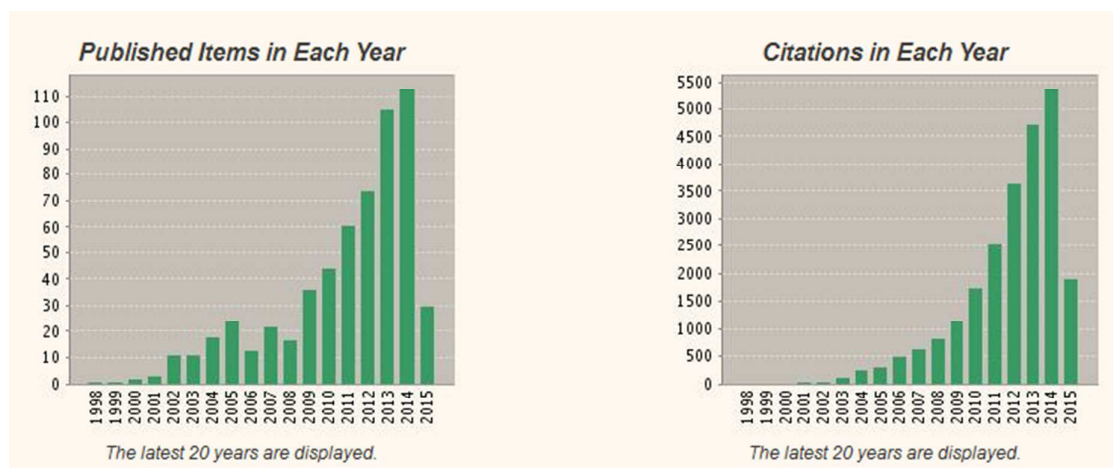
Fig. 2 Number of publications and citations annually dealing with electrolyte complexes in DSSCs showing the exponential growth in interest in recent years (data collected with topic of complex electrolyte in DSSC from Web of Science, June 8, 2015).

By employing electron transfer mediator systems such as $[Co(dtb)_3]^{2+/3+}$, it is feasible to investigate new options for addressing the distance between charge collecting substrates. It is a significant factor in cell's performance that is unavailable with the I^-/I_3^- mediator system.[35] By employing transparent conducting metal-oxide electrodes and operating two cells in optical tandem in $[Co(dtb)_3]^{2+/3+}$-mediated DSSCs, both I_{sc} and the overall cell efficiency can be increased.

Nakade et al. reported roles of electrolytes in DSSCs on charge recombination using two different cobalt complex redox couples of $Co^{II}(abpn)$ (abpn= propylene-1,2-bis(o-iminobenzylideneaminato)) and $[Co(dtb)_3]^{2+/3+}$.[36] It was found that the increase of Co^{II} complex concentrations leads to the density reduction of dye cations, which will improve I_{sc} value. Due to the slow charge-transfer kinetics and cationic nature of the Co-complex redox couples, they are more likely to experience recombination with photoelectrons from TiO_2. Using Li^+ as an electrolyte additive resulted an increase in the electron lifetime for a specific Co(II/III) electrolyte, which was attributed to the decreased local concentration of Co(III) on TiO_2 surface. Additionally, TBP (tert-butyl pyridine) with Li^+ increased I_{sc} and the electron lifetime. Since TBP facilitates the charge transfer from Co(II) to the dye cation, by change of the reorganization energy between Co(II) and Co(III).

Nelson et al. studied the diffusion of $[Co(dtb)_3]^{2+/3+}$ in DSSCs, which clearly proved that diffusion of $[Co(dtb)_3]^{3+}$ is dramatically slower than that of I_3^- under operating DSSC conditions.[37] This difference may be attributed to the greater size and slower bulk diffusion of $[Co(dtb)_3]^{2+/3+}$, greater viscosity of cobalt complex solutions, and a possible electrostatic surface interaction of $[Co(dtb)_3]^{2+/3+}$ within the TiO_2 film.

In order to minimize the recombination between photoinjected electrons and Co(III) species, a thin Al_2O_3 blocking layer was used over the mesoporous TiO_2 surface.[38] The overall efficiency increment is more than double, reaching from 0.94% (TiO_2) to 2.48% (TiO_2 + Al_2O_3) under 300 W m^{-2} AM 1.5 illumination. In addition, further investigation of $[Co(dtb)_3]^{2+/3+}$, $[Co(dmb)_3]^{2+/3+}$ (Table 1), and $[Co(bpy)_3]^{2+/3+}$ mediators progressed with Al_2O_3 coated TiO_2 films, which decreases the rate of recombination for all electrolytes investigated, by Klahr and Hamann.[39] In order to determine the reason of remarkable variations between photovoltaic parameters, the impedance measurements were performed on DSSCs based on these cobalt bipyridyl redox couples. The differences in the lifetimes (recombination kinetics) of cobalt redox couple DSSCs

have a coherent correlation with the differences in IPCEs. The trend of IPCEs for DSSCs and the lifetimes at a given electrode potential was found to decrease in the order: $[Co(dtb)_3]^{2+/3+}$ > $[Co(dmb)_3]^{2+/3+}$ > $[Co(bpy)_3]^{2+/3+}$. The order are strong evidence that the external quantum efficiencies of DSSCs with cobalt polypyridyl redox couples are limited by recombination.[39] With the dye $[Ru(bpy)_2(4,4'-dicarboxy-bpy)](PF_6)_2$, cobalt redox couples presented better dye regeneration abilities compared to I^-/I_3^-, and this is an advantage of Co-complex shuttles. These results display that the structures of the Co redox shuttles are also very important to the DSSCs. The tert-butyl units of the ligands in the complex can act as spacers, and so decrease the electronic coupling by a factor of 20 relative to methyl-substituted ones. Moreover, $[Co(dmb)_3]^{2+/3+}$ couple can generate a significant external quantum yield compared to $[Co(dtb)_3]^{2+/3+}$. Nevertheless, the photovoltaic performances of both are inhibited by mass transport of the oxidized species. In another work based on $[Co(phen)_3](ClO_4)_2$ (phen= 1,10-phenanthroline) and its derivatives, similar behavior was observed.[40]

Feldt et al. developed a suitable combination of cobalt polypyridine complexes and organic sensitizers (D35 and D29) to overcome the mass transport and recombination limitations associated with cobalt polypyridine redox electrolytes.[25] Organic dyes have typically higher extinction coefficients rather than the standard ruthenium sensitizers, that use ionic liquids or solid-state hole conductors. Since, they allow good light harvesting efficiencies using thinner TiO_2 films. In a thinner TiO_2 film, the current is clearly limited by slow mass transport through the mesoporous TiO_2 film and the risk of recombination will be loosed. Both of cobalt polypyridine mediators and the organic dye structures showed significant effects on the efficiencies of DSSCs. An overall conversion efficiency of 6.7% was obtained with DSSC sensitized with D35 and employing a $[Co(bpy)_3]^{2+/3+}$-based electrolyte. While the I^-/I_3^- yields efficiency of 5.5% under 100 mW cm^{-2} AM1.5 G illumination. The high efficiency obtained with D35 was related to the efficient blocking of the recombination by the bulky alkoxy substituents on the dye. However, for D29 featuring with N,N-dimethylanilinyl units, the recombination process is easily proceeded between electrons in TiO_2 and Co(III) species in the electrolyte. In addition, the photocurrent and photovoltage of the device was improved by cobalt redox system with the highest diffusion coefficients and more suitable redox potentials. Also, DSSCs sensitized with organic dyes in the presence of cobalt-based mediators are promising candidates for indoor applications. This

happens because the voltage and efficiency remain high under low light intensities.[25] Additionally, the surface modification of TiO_2 thin film electrodes by fluorine plasma treatment[41] and utilization of different low cost carbon materials as counter electrodes[42] were investigated with employing the Co(II/III) redox shuttle and the organic D35 sensitizer. Mesoporous TiO_2 microbeads were also tested as working electrode in DSSCs based on $[Co(bpy)_3]^{2+/3+}$ electrolyte, which power conversion efficiencies up to 6.4% were obtained with D35.[43]

Anyway, D35 harvests only sunlight below 620 nm, which limits I_{sc} to 10–11 mA cm^{-2}. Tsao et al. achieved an impressive efficiency of 9.6% with modifying this sensitizer by introducing a cyclopentadithiophene bridging unit and improving its red absorption.[27] Due to the higher redox potential, the lower light absorption and an unexpected broadening of the IPCE in the red region of the spectrum, the new Y123 dye achieves higher conversion efficiencies with the Co(II/III) redox couple rather than the analogous iodine-based electrolyte. Additionally, C243-sensitized solar cells with a $[Co(bpy)_3]^{2+/3+}$ redox shuttle attained an efficiency of 8.9%.[44]

In addition, two new organic D-π-A dyes including NT35 and G220, were synthesized which comprise BPTPA (N-(2',4'-bis(hexyloxy)-[1,1'-biphenyl]-4-yl)-N-(4-bromophenyl)-2',4'-bis(hexyloxyy)-[1,1'-biphenyl]-4-amine) donor. Both dyes exhibited greater IPCE response with cobalt-based redox shuttles, compared to the classical I^-/I_3^- electrolyte.[45] Among these dyes, G220 showed the best photovoltaic performance. The results proved that organic dyes based on this bulky BPTPA donor are promising candidates for cobalt-based DSSCs, due to suppressing the electron recombination between the TiO2 surface and the redox oxide species.

Moreover, the effect of 4-TBP in triphenylamine-based organic DSSCs was examined using the $[Co(bpy)_3]^{2+/3+}$ redox shuttle.[46] The higher amount of TBP in mediator increases the viscosity of electrolyte and hence slows down the diffusion of Co(III) species. This is a unique observation for Co(II/III) electrolyte which is not detected in I^-/I_3^- electrolyte. Increasing TBP concentration improved the open-circuit potential, which could be attributed to the reduced interfacial recombination as well as a negative shift in the conduction band level of TiO_2.

Another notion in the application of Co-complexes is to develop the mediator mixture, which proposes that the electrolyte could employ two or more than two redox couples to achieve the multistep electron transfer processes. Thus the electron recombination decreases to improve the electron-collection efficiency.[47-50] An easily accessible homoleptic Ru complex containing dissymmetrical bipyridine in the presence of the mediator mixture of $[Co(dtb)_3]^{2+}$ and $[Fe(dmb)_3]^{2+}$ reached the best results, which offered an adequate balance between regeneration of the dye and back recombination with photoinjected electrons in TiO_2.[49] Despite a lower regeneration kinetic, the bulky effect of $[Co(dtb)_3]^{2+}/[Fe(dmb)_3]^{2+}$, led to slower recombination rates and better overall performance.[49] Using these mediators, the related dye[49] displayed interesting performances (65%) slightly lower than those obtained for bis-heteroleptic dyes[48] (68 and 75% IPCE, respectively). Combination of the mediators based on cobalt complexes and adequate co-mediators based on iron complexes can be used to improve the electron-collection efficiency in Ru-thienyltpy-sensitised solar cells.[50] In combination with Ru-based dye, the charge-collection efficiency was improved by efficient dye regeneration and retarded recombination losses. Additionally, chronocoulometry experiments demonstrated that the efficiency of the regeneration cascade is critically dependent on the ability of the Co(II) complex to intercept Fe(III) centers, as clearly indicated. The relatively low concentration of Fe-complex could be rapidly captured by Co complex after the dye regeneration, thus preventing the injected electrons in the semiconductor from recombining with the oxidized Fe-complex. The maximum IPCEs of

65% and 20% were obtained with Co(dtb)/Fe(dmb) and I^-/I_3^-, respectively.

DSSCs with power conversion efficiencies of up to 6.5% were fabricated using a $[Co(bpy)_3]^{2+/3+}$ redox electrolyte with the Z907 sensitizer.[51] This better performance relative to benchmark sensitizer N719 was explained by near-IR transmittance measurements in conjunction with the electrochemical impedance spectroscopy. The results showed that the small-perturbation electron diffusion length (L_n) is significantly longer in Z907 cells in comparison with that in N719 cells, which can explain differences in performance. In addition, it is demonstrated that the longer L_n in Z907 cells is caused by inhibited recombination, as opposed to faster transport, and possible reasons for this are discussed.
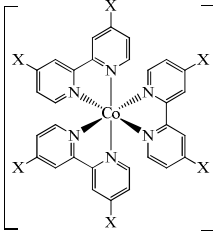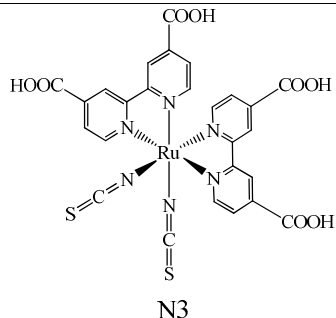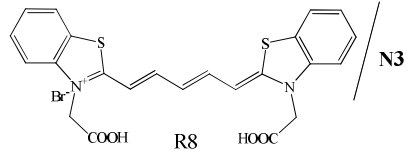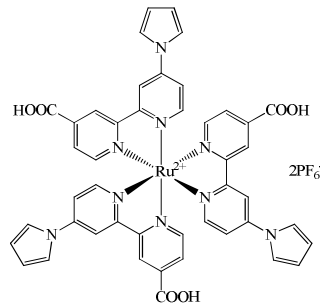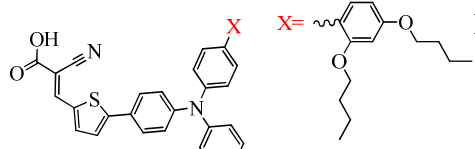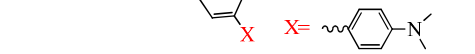
Moreover, applying of bulky substitutions in a new heteroleptic Ru(II)-based complex, TT-230, was investigated to obtain high open-circuit potential in DSSCs with cobalt redox shuttles.[52] The electrolytes based on cobalt complexes have revealed substantial advantages in terms of achievable V_{oc} compared to the standard I^-/I_3^- redox mediators. These merits of the cobalt mediators were realized with a porphyrin dye, reaching a V_{oc} greater than 1 V in DSSC,[53] which could not be attained with Ru(II) complexes, due to the enhanced recombination. Anyway, TT-230 dye provided an example of a bulky Ru(II)-dye reaching high V_{oc} in DSSC in combination with the Co(II/III) redox couple.[52]
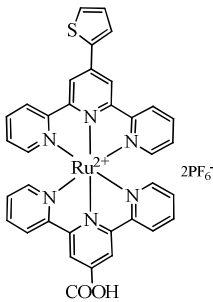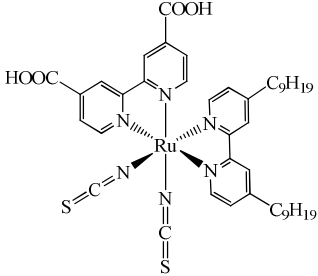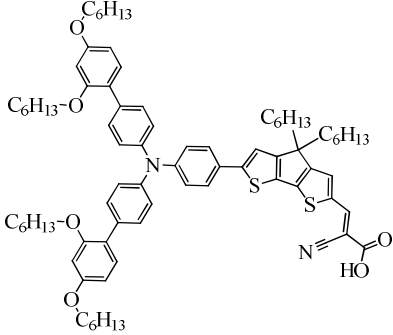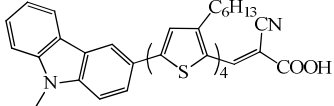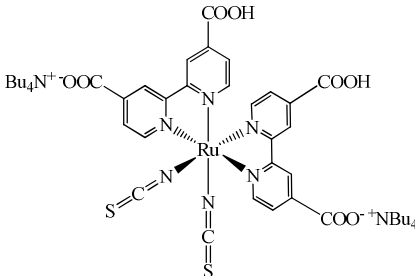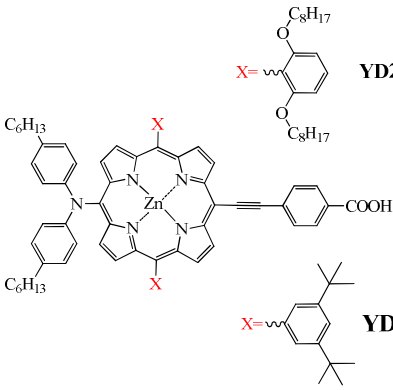
However, the disadvantages of cobalt-based electrolytes includes rapid recombination of electrons in TiO_2 conduction band with the oxidized Co(III) species, mass transport problems in the mesoporous TiO_2 electrode and low diffusion coefficients. Thus, different TiO_2 films are used to suppress recombination and improve redox transport. Kim et al. developed a facile approach to solve the mass transport problem in $[Co(bpy)_3]^{2+/3+}$ electrolyte system by tuning the porosity of mesoporous TiO_2 films. With increasing the porosity from 0.52 to 0.59 despite the decreasing of 23% in dye loading, photocurrent density was improved by nearly two times. MK-2-sensitized solar cell showed an efficiency of 5.5% at 1 sun.[54] In addition, $[Co(dtb)_3]^{2+/3+}$ has been used resulting 2.4% efficiency with N719-sensitized 35 μm TiO_2 nanotubes.[55]
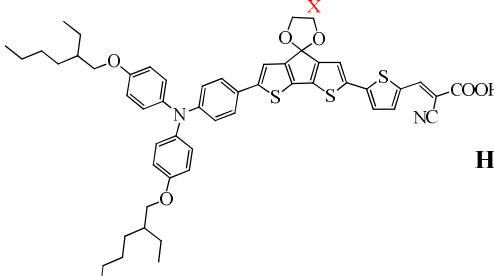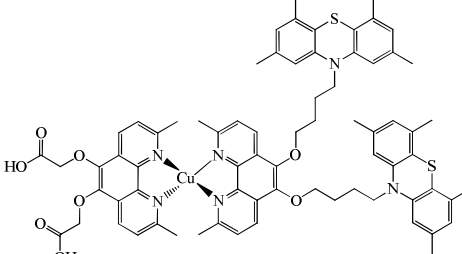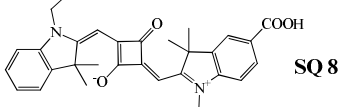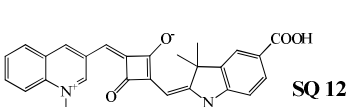
Highly porous counter electrodes based on poly(3,4-ethylenedioxythiophene) (PEDOT) displayed much better electrocatalytic activity for $[Co(bpy)_3]^{2+/3+}$ redox couple. Also, due to both charge-transfer resistance and stability, the GNP film was better than those of the traditional Pt-based electrode under prolonged potential cycling. Higher efficiencies obtained when PEDOT, a highly porous cathode based on poly(3,4-ethylenedioxythiophene), was employed as a catalyst on the counter electrode. It shows much lower charge transfer resistance for $[Co(bpy)_3]^{2+/3+}$ and $[Co(phen)_3]^{2+/3+}$ redox shuttles.[56] The fabricated solar cell with this electrode, sensitized with dye Y123 and the $[Co(bpy)_3]^{2+/3+}$ redox couple indicated an excellent power conversion efficiency of 10.3%. However, different PEDOT-based counter electrodes in the presence of Co(II/III) polypyridine redox mediators were compared to Pt- and Al-coated electrodes in order to evaluate the potential use of PEDOT counter electrodes in DSSCs.[57] Also, two different kinds of nanocomposites, TiC-PEDOT and TiN-PEDOT, utilizing a Co(II/III) polypyridyl redox mediator and MK2 dye showed equivalent or higher photovoltaic conversion efficiencies compared to cells with pristine PEDOT or Pt coated electrodes.[58]

Electron-transfer reactions from TiO_2 nanoparticle films to $[Co(dmb)_3]^{3+}$ and $[Ru(bpy)_2(NMI)_2]^{3+}$ (NMI= N-methylimidozole) redox shuttles through both measurements and modeling showed an excellent agreement between the modeled and measured lifetimes.[59] The highly positive redox shuttle $[Ru(bpy)_2(NMI)_2]^{2+/3+}$ are also used to probe the details of dark current density in DSSCs.[60]
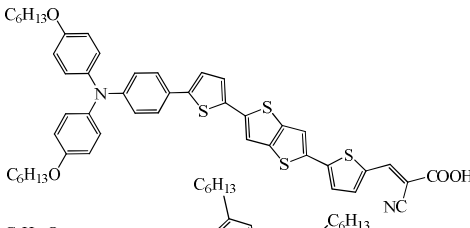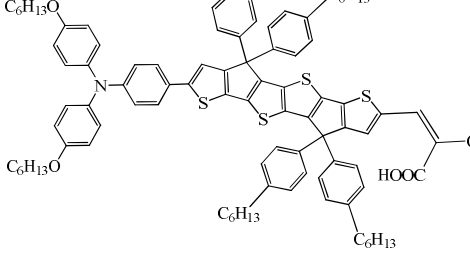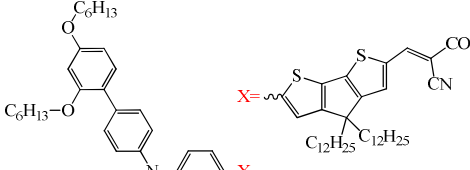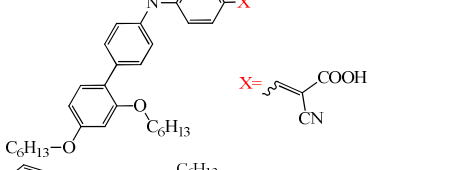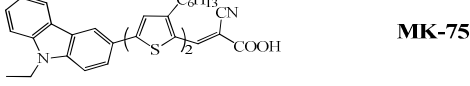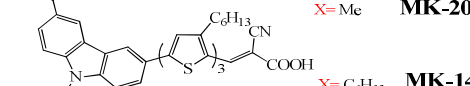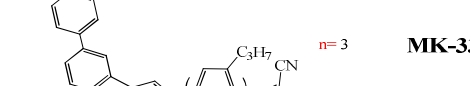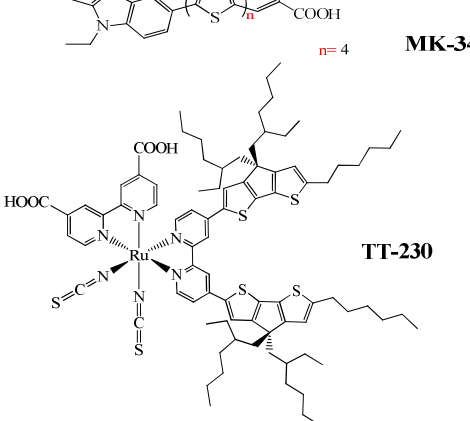
Table 1 Photovoltaic parameters for DSSCs based on Co-bipyridine mediators in combination with different dyes. For comparison the corresponding parameters for DSSCs containing the standard I^-/I_3^- redox couple are also reported, when available.

$$[Co(X\text{-}bpy)_3]^{2+/3+}$$
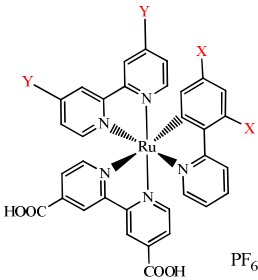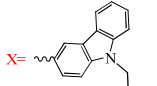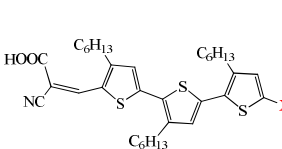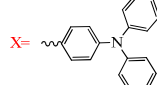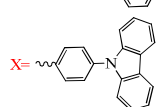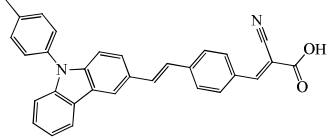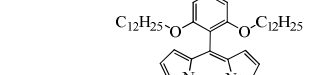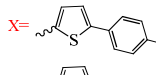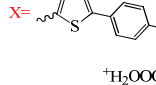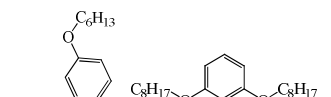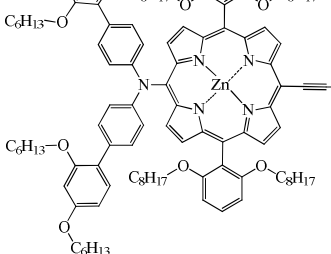
X= H $[Co(bpy)_3]^{2+/3+}$
X= metthyl $[Co(dmb)_3]^{2+/3+}$
X= tert-butyl $[Co(dtb)_3]^{2+/3+}$
X= 3-pentyl $[Co(d3pb)_3]^{2+/3+}$
X= nonyl $[Co(dnb)_3]^{2+/3+}$
X= phenyl $[Co(dpb)_3]^{2+/3+}$
X= 1,3-dimethyl-1*H*-imidazol-3-ium hexafluorophosphate $[Co((MeIm\text{-}Bpy)PF_6)_3]^{2+/3+}$

Electrolyte	Sensitizer	V_{oc} (V)	I_{sc} (mA cm^{-2})	FF	IPCE (%)	η (%)	Ref.
$[Co(dtb)_3]^{2+/3+}$	N3	0.44	4.82	0.62	-	1.30	
$[Co(d3pb)_3]^{2+/3+}$		0.47	1.47	0.59	-	0.41	33
$[Co(dnb)_3]^{2+/3+}$		0.43	0.89	0.59	-	0.22	
$[Co(dpb)_3]^{2+/3+}$		0.40	0.97	0.49	-	0.19	
$[Co(dtb)_3]^{2+/3+}$	R8	0.49	2.44	-	-	0.67	35
$[Co(bpy)_3]^{2+/3+}$	$[Ru(bpy)_2(4,4'\text{-dicarboxy-bpy})](PF_6)_2$	0.53	4.1	0.60	25	1.3	
$[Co(dmb)_3]^{2+/3+}$		0.47	6.9	0.41	43	1.3	39
$[Co(dtb)_3]^{2+/3+}$		0.50	7.4	0.32	63	1.2	
I^-/I_3^-		0.56	10.1	0.66	80	3.7	
$Co(dtb)_3^{2+}/Fe(dmb)_3^{2+}$		0.36	0.25	0.61	65	5.4	49
I^-/I_3^-		0.37	0.18	0.52	-	3.4	
$[Co(bpy)_3]^{2+/3+}$	D35	0.92	10.7	0.68	90	6.7	
I^-/I_3^-		0.91	9.38	0.65	90	5.5	25
$[Co(dmb)_3]^{2+/3+}$	D29	-	-	-	-	2.6	

X= D35
X= D29
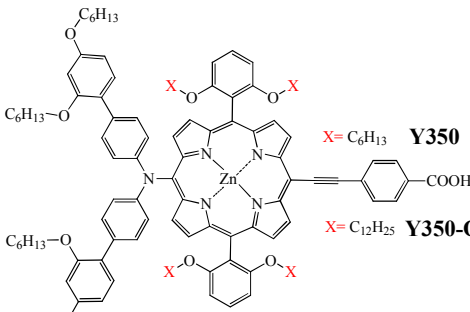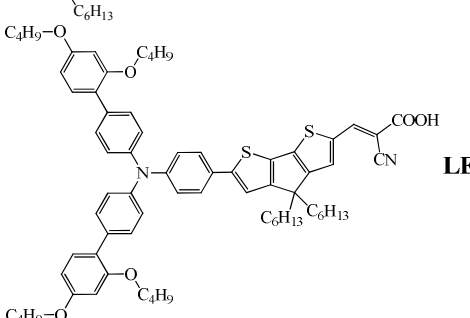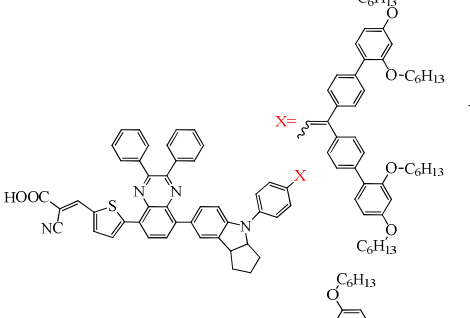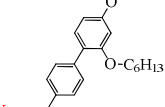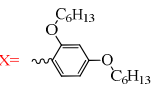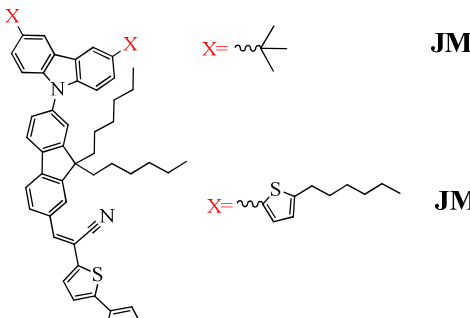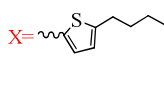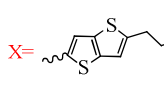
	Dye						Ref.
$[Co(dtb)_3]^{2+/3+}$ / $[Fe(4,4'\text{-dimethyl-2,2'-bipyrindine})_3]^{2+/3+}$		-	-	-	65	-	50
$[Co(bpy)_3]^{2+/3+}$ / I^-/I_3^-	Z907	0.74 / 0.79	14.0 / 15.9	0.62 / 0.61	- / -	6.5 / 7.7	51
$[Co(bpy)_3]^{2+/3+}$ / I^-/I_3^-	Y123	0.86 / 0.76	14.6 / 13.6	0.70 / 0.70	92 / -	8.8 / 7.2	27
$[Co(bpy)_3]^{2+/3+}$	MK-2	0.74	12.6	0.59	-	5.5	54
$[Co(dtb)_3]^{2+/3+}$ / I^-/I_3^-	N719	0.53 / 0.66	9.8 / 11.56	0 46 / 0.55	- / -	2.38 / 4.20	55
$[Co(bpy)_3]^{2+/3+}$	YD2-o-C8	0.97	17.3	0.71	-	11.9	53
	YD2	0.83	14.9	0.69	-	8.4	
	YD2-o-C8/Y123	0.94	17.66	0.74	-	12.3	

ARTICLE

Electrolyte	Dye						Ref
$[Co(bpy)_3]^{2+/3+}$ I^-/I_3^-	D9L6	0.69 / 0.64	10.7 / 11.6	0.72 / 0.71	- / -	5.32 / 5.30	
$[Co(bpy)_3]^{2+/3+}$ I^-/I_3^-	D21L6	0.85 / 0.7	12.3 / 12.9	0.63 / 0.66	- / -	6.63 / 6.0	61
$[Co(bpy)_3]^{2+/3+}$ I^-/I_3^-	D25L6	0.85 / 0.71	10.8 / 11.2	0.63 / 0.67	- / -	5.51 / 5.30	
$[Co(bpy)_3]^{2+/3+}$ I^-/I_3^-	HIQ7	0.75 / 0.62	8.38 / 6.24	0.65 / 0.64	- / -	4.04 / 2.44	62
$[Co(dtb)_3]^{2+/3+}$		0.57	0.54	0.69	-	-	63
$[Co(dmb)_3]^{2+/3+}$ $[Co(bpy)_3]^{2+/3+}$ $[Co(phen)_3]^{2+/3+}$ I^-/I_3^-	SQ 8	0.32 / 0.34 / 0.32 / 0.72	1.99 / 1.45 / 0.84 / 7.22	- / - / - / -	- / - / - / -	0.26 / 0.18 / 0.08 / 3.28	64
$[Co(dmb)_3]^{2+/3+}$ $[Co(bpy)_3]^{2+/3+}$ $[Co(phen)_3]^{2+/3+}$ I^-/I_3^-	SQ 12	0.24 / 0.20 / 0.21 / 0.61	1.19 / 0.37 / 0.13 / 6.61	- / - / - / -	- / - / - / -	0.09 / 0.02 / 0.01 / 2.29	
$[Co(bpy)_3]^{2+/3+}$ I^-/I_3^-	Dye-O	0.73 / 0.71	11.7 / 10.1	0.70 / 0.64	- / -	6.1 / 4.6	65
$[Co(bpy)_3]^{2+/3+}$ I^-/I_3^-	Dye-S	0.83 / 0.80	10.8 / 10.3	0.70 / 0.74	- / -	6.3 / 6.2	
$[Co((MeIm-Bpy)PF_6)_3]^{2+/3+}/I^-$ I^-/I_3^-	N719	0.70 / 0.62	8.42 / 7.83	0.71 / 0.72	- / -	8.29 / 6.97	66

X= CH₃ → D9L6
X= C_6H_{13} → D21L6
X= $C_{12}H_{25}$ → D25L6

X= O Dye-O
X= S Dye-S

RSC Advances Accepted Manuscript

$[Co(bpy)_3]^{2+/3+}$	**C242**	0.72	12.92	0.76	-	7.0	44
	C243	0.75	15.67	0.76	-	8.9	
$[Co(bpy)_3]^{2+/3+}$ I^-/I_3^-	**G220**	0.87	14.8	0.71	-	9.06	45
		0.76	13.1	0.71	-	6.97	
$[Co(bpy)_3]^{2+/3+}$ I^-/I_3^-	**NT35**	0.93	5.80	0.70	-	8.92	
		0.79	7.96	0.74	-	4.70	
	MK-75	0.72	8.15	0.72	-	4.2	
	MK-20	0.79	10.8	0.71	-	6.0	
$[Co(bpy)_3]^{2+/3+}$	**MK-14**	0.80	11.0	0.71	-	6.3	67
	MK-33	0.83	11.7	0.69	-	6.6	
	MK-34	0.83	11.5	0.67	-	6.4	
$[Co(bpy)_3]^{2+/3+}$	**TT-230**	0.77	3.3	0.73	-	1.8	52

RSC Advances Accepted Manuscript

Mediator	Dye	V_{oc}	J_{sc}	FF		PCE	Ref
$[Co(dmb)_3]^{2+/3+}$	X=H, Y=H **1d**	0.51	5.33	0.71	-	1.91	
	X=H, Y=C$_9$H$_{19}$ **ss-14**	0.51	5.53	0.69	-	1.94	[68]
	X=F, Y=C$_9$H$_{19}$ **ss-22**	0.57	7.44	0.68	-	2.86	
$[Co(bpy)_3]^{2+/3+}$	**MK-1**	0.78	11	0.72	-	6.0	
	MK-31	0.76	12	0.69	-	6.1	[69]
	MK-88	0.81	10	0.70	-	5.8	
	MK-90	0.73	8.1	0.69	-	4.1	
$[Co(bpy)_3]^{2+/3+}$ I^-/I_3^-	**SK1**	0.72 / 0.63	12.04 / 12.22	0.65 / 0.61	60 / 62	5.7 / 4.7	[70]
$[Co(bpy)_3]^{2+/3+}$	X= —COOH **LD14**	0.81	13.23	0.73	-	7.93	
	LW5	0.81	12.66	0.75	-	7.75	[71]
	LW6	0.76	10.66	0.74	-	6.09	
$[Co(bpy)_3]^{2+/3}$	**SM371**	0.96	15.9	0.79	80	12.0	[72]
	SM315	0.91	18.1	0.78	80	13.0	

ARTICLE

$[Co(bpy)_3]^{2+/3+}$	X= C_6H_{13} **Y350**	0.94	17.2	0.74	-	12.0	73
	X= $C_{12}H_{25}$ **Y350-OC12**	0.97	16.0	0.74	-	11.5	
$[Co(bpy)_3]^{2+/3+}$	**LEG4**	0.96	13.40	0.65	-	8.4	74
$[Co(bpy)_3]^{2+/3+}$ (Au + graphene cathode)	**YA422**	0.89	16.25	0.74	90	10.65	75
$[Co(bpy)_3]^{2+/3+}$ (graphene cathode)	X= **YA421**	0.8	15.58	0.71	90	8.84	
$[Co(bpy)_3]^{2+/3+}$ I^-/I_3^-	X= **JM-1**	0.71 / 0.64	7.8 / 9.7	0.61 / 0.63	- / -	3.4 / 3.9	76
$[Co(bpy)_3]^{2+/3+}$ I^-/I_3^-	X= **JM-2**	0.74 / 0.67	7.2 / 7.7	0.70 / 0.73	- / -	3.7 / 3.8	
$[Co(bpy)_3]^{2+/3+}$ I^-/I_3^-	X= **JM-3**	0.64 / 0.61	6.6 / 6.9	0.65 / 0.63	- / -	2.7 / 2.7	
$[Co(bpy-pz)_2]^{2+/3+}$	**JM-1**	0.87	8.0	0.61	-	4.3	76
	JM-2	0.92	5.9	0.70	-	3.7	
	JM-3	0.80	4.4	0.67	-	2.4	

Electrolyte	Dye	V_{oc}	J_{sc}	FF		η	Ref
$[Co(bpy)_3]^{2+/3+}$ I^-/I_3^-	X= H, Ar= Ph, n= 2 **JK-318**	0.94 / 0.80	9.06 / 8.62	0.73 / 0.77	- / 80	6.25 / 5.31	
$[Co(bpy)_3]^{2+/3+}$ I^-/I_3^-	X= H, Ar= InT, n= 1 **JK-319**	0.93 / 0.79	9.33 / 8.90	0.74 / 0.77	- / 80	6.38 / 5.41	77
$[Co(bpy)_3]^{2+/3+}$ I^-/I_3^-	X= OC$_6$H$_{13}$, Ar= InT, n= 1 **JK-320**	0.94 / 0.83	9.85 / 9.16	0.72 / 0.78	- / 80	6.66 / 5.88	
	DT-1	0.80	16.08	0.66	-	8.57	
$[Co(bpy)_3]^{2+/3+}$	**DT-2**	0.9	15.35	0.64	-	7.74	1

InT= (structure)

Using the standard $[Co(bpy)_3]^{2+/3+}$ redox couple and a newly designed donor-π-bridge-acceptor zinc porphyrin, YD2-o-C8, comprising two alkyl chains and four alkoxy chains on the ligand of the complex, an efficiency of 11.9% was achieved.[53] The alkyl chains greatly retard the rate of interfacial back-electron transfer to Co(III) mediator, which enables attainment of strikingly high photovoltages of 1 V. Remarkably, the co-sensitization of YD2-o-C8 with the organic D-π-A dye, Y123, yielded an efficiency of 12.3% when used in conjunction with the $[Co(bpy)_3]^{2+/3+}$-based redox electrolyte.[53] The improvement in photovoltaic performance over the devices containing an iodide redox mediator was due to an increase in V_{oc}.[78] This system generated a strikingly high photovoltage close to 1 volt and has an impressive photocurrent density, due to the specific molecular design of YD2-o-C8. This greatly retards the rate of interfacial back electron transfer from the conduction band of the TiO$_2$ film to Co(III) mediator. A research is currently focused in this direction to improve the performance of various sensitizers with cobalt-based redox electrolytes.[78] In addition, transparent conductive oxide-less back contact DSSCs using YD2-o-C8 dye employing cobalt redox shuttle gave the power conversion efficiency of 4.89% under simulated solar irradiation. While that of the iodine based electrolyte was found to be 3.05%.[79]

However, by modifying the YD2-o-C8 porphyrin core with the bulky bis(2′,4′-bis(hexyloxy)-[1,1′-biphenyl]-4-yl)amine donor (SM371) and with incorporation of the proquinoidal benzothiadiazole (BTD) unit into SM371 the dye SM315 was afforded.[72] Fig. 3 illustrates the I–V curve for the two devices measured under AM 1.5G illumination (1,000 W m⁻² at 298 K). Fabrication of DSSCs utilizing the $[Co(bpy)_3]^{2+/3+}$ redox couple and

SM315 showed a record of η= 13.0% at full sun illumination without the requirement of co-sensitizer. The results showed that the SM315 is a very stable dye and not prone to degradation, even if exposed to intense sunlight for long illumination times. During the 500 h of light soaking, devices employing SM315 underwent over one million turnovers without showing any significant loss in stability.

Moreover, to understand the effect of the alkoxy groups on the zinc porphyrin dyes in conjunction with $[Co(bpy)_3]^{2+/3+}$ redox couple, two new dyes denoted as Y350 and Y350-OC12 by modifying the structure of YD2-o-C8 were used in DSSCs and achieved a power conversion efficiency of up to 12.0% under standard conditions.[73]

A combined experimental and computational investigation was reported by Mosconi et al. to understand the nature of the interactions between cobalt redox mediators and TiO$_2$ surfaces sensitized by ruthenium and organic dyes. Also their impact on the performance of the corresponding DSSCs were investigated.[61] Both N719- and Z907-based DSSCs exhibited an increased lifetime in iodine-based electrolyte compared to the cobalt-based redox shuttle. However the D21L6 and D25L6 organic dyes, endowed with long alkoxy chains, showed no significant change in the electron lifetime regardless of employed electrolyte and delivered a high photovoltaic efficiency of 6.5% with a cobalt electrolyte. Additionally, a series of Co(II/III) complexes were investigated to gauge the impact of ligand substitution and metal coordination on the High Spin/Low Spin energy difference as well as reorganization energies. The results allow tracing the structure/property relations required for further development of cobalt electrolyte DSSCs.[61]
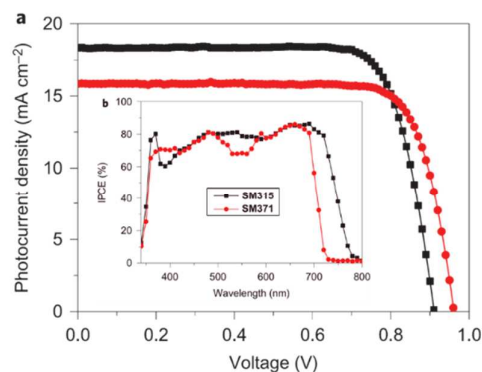
Fig. 3 Photovoltaic performance (a) and IPCE curves (b) of devices made with SM371 and SM315. Reproduced with permission from ref. 72. Copyright 2014, Nature Publishing Group.

Moreover, the similar experimental and computational investigations were carried out to understand the nature of the interfaces between dye-sensitized TiO_2 and cobalt-based electrolyte in the presence of chenodeoxycholic acid (CDCA) as a surface co-adsorbent and additive in combination with N719 and Z907 dyes.[80] For both dyes, the concomitant use of CDCA in the dye bath and electrolyte solution was led to a significant improvement, which is in agreement with that reported by Daeneke et al.[8] for the related Fc/Fc^+ redox couple.

A novel donor-π-acceptor organic dye (HIQ7) was used in DSSCs with a cobalt redox shuttle. HIQ7 comprises the electron-rich group for harvesting a broad spectrum of white light, the bulky group to suppress charge recombination and also an electron-donating group for facilitating dye regeneration.[62] The sensitized cells with HIQ7 along with a cobalt electrolyte indicated broad incident monochromatic photon-to-current conversion efficiency spectra, which cover the entire visible range with an overall conversion efficiency of 4.04%. This value was 1.65 times greater than that was observed with an iodine electrolyte.

Testing a series of metals including Al, Cu, Zn, Ni, Stainless steel (StS) 304, StS 321, and Ti as a substrate for a counter electrode in DSSC exhibited that some metals can be a suitable choice to apply with cobalt electrolyte.[81] The results showed that Stainless steels 304 and 321 as well as Ni and Ti suit well to the counter electrodes in DSSCs with Co-mediator. In these metals, both lifetime and efficiency were similar to the reference cells on conducting glass substrates. In contrast, the cells with Al, Zn and Cu substrates suffered from both poor stability and low efficiency (Fig. 4), in which the SEM analysis revealed clear marks of corrosion for these three metals.
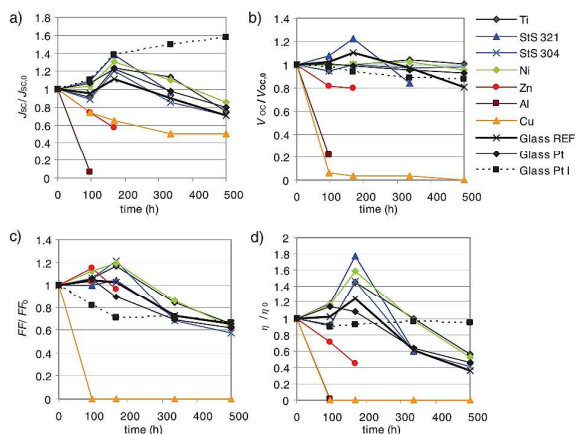
Fig. 4 Normalized aging data (i.e. the aging data divided by initial performance data for each cell) in light soaking 1 Sun at 40 °C. The cells are kept in open circuit during the light soaking. Notation "glass" refers to FTO glass. Reproduced with permission from ref. 81. Copyright 2013, Electrochemical Society.

Ashbrook and Elliott demonstrated that bis(2,9-dimethyl-1,10-phenanthroline) Cu(I)-based chromophores paired with $[Co(dtb)_3]^{2+/3+}$ mediator can function expertly as dyes in DSSCs.[63] These dyes have a number of photophysical similarities with trisbipyridine-Ru(II). The similarities include a strong MLCT absorption in the visible, a relatively long excited-state lifetime, and a thermally equilibrated MLCT state that is a potent reductant. In addition, there are significant differences including the lability of the Cu(I) dyes in solution and their long-term incompatibility with the most common mediator system, I^-/I_3^-. $[Cu(KbindDMP)(tmpDMP)]^+$ showed the best performance among these complexes (I_{sc}= 0.54 mA cm^{-2}, V_{oc}= 570 mV, FF= 0.69).

Impedance spectroscopy was employed over a range of temperatures to describe the electron storage, transport, and recombination in efficient DSSCs based on $[Co(bpy)_3]^{2+/3+}$ redox mediator. The corresponded mediator could contain either the amphiphillic ruthenium sensitizer Z907 or the state-of-the-art organic sensitizer Y123.[82] The temperature dependency of the electron-transport resistance displayed that the transport occurs via the states at energies lower than commonly assumed for the TiO_2 conduction band edge. The results also showed that the nature of the sensitizing dye controls the predominant recombination route: via band gap states for Z907 and the conduction band for Y123. This could be the main reason for the superior performance of the dyes. Moreover, the DSSC devices based on new D-π-A porphyrin sensitizers LW5 and LW6 with $[Co(bpy)_3]^{2+/3+}$ redox couple showed efficiencies of 7.8% and 6.1%, respectively.[71]

A series of DSSCs were reported with two types of squaraines (SQs) including indole (SQ 8) and quinoline (SQ 12) as sensitizer and three different Co-based complexes with different oxidation potentials including $[Co(dmb)_3]^{2+/3+}$, $[Co(bpy)_3]^{2+/3+}$, and $[Co(phen)_3]^{2+/3+}$. This investigate the photodynamics of the different electron transfer reactions.[64] The results showed that that the electron recombination with the oxidized redox species is faster with the Co-based compared to the I^-/I_3^- electrolytes for both SQs. This indicates that these SQs are not bulky enough to avoid the interaction between the Co(III) species and the electron in the TiO_2 nanoparticles. Additionally, the regeneration rate constants and efficiencies are noticeably smaller for the cells with the different Co-based electrolytes relative to those with the I^-/I_3^- pair. Consequently, utilization of Co-based electrolytes in these two SQs is unfavorable to the overall efficiency of the cell, since $-\Delta G_{reg}$ values of below 0.4 eV do not give complete regeneration efficiency.

To explore the potential mismatch between the complex mediators and N719 dye, some important cobalt redox couples with redox potentials ranging between 0.25 and 0.86 V vs NHE, are shown in Fig. 5.
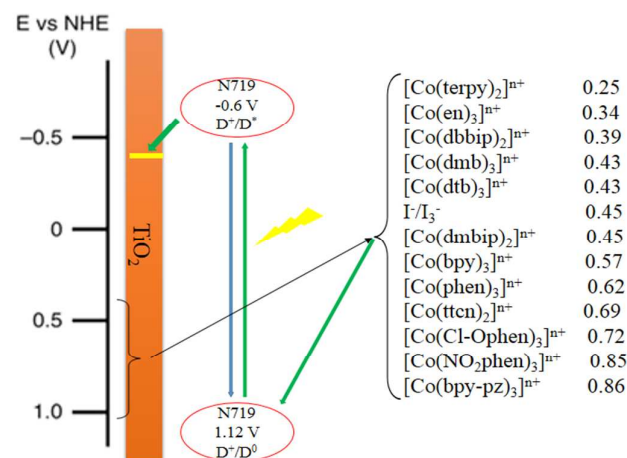
Fig. 5 Energy level diagram showing the approximate redox potentials of N719 and Co complex electrolyte relative to the normal hydrogen electrode.

Two donor-acceptor or push-pull type organic dyes, Dye-O and Dye-S, were synthesized and tested in solar cell devices employing both I^-/I_3^--based and $[Co(bpy)_3]^{2+/3+}$ redox mediators.[65] It was shown that the identity of the heteroatom can have a profound effect on dye regeneration, and in turn the V_{oc} as the S atoms increase the rate of the reaction between the oxidized dye and the redox mediator by 25-fold with I^-/I_3^- electrolytes, and 3-fold with $[Co(bpy)_3]^{2+/3+}$. Therefore, the careful design of molecular dyes can lead to an optimization of interactions with the electrolytes that cause further enhancements in dye regeneration.

With the aim of fabrication and characterization of Co(II/III) complex redox shuttle-based organic solvent-free ionic liquid electrolyte DSSCs, Xu et al. synthesized an imidazolium functionalized Co-tris(bipyridyl) complex redox mediator ($[Co((MeIm-Bpy)PF_6)_3]^{2+/3+}$) (Table 1) with high redox potential and good solubility in ionic liquid electrolyte and applied in ionic liquid electrolyte DSSCs.[66] The redox potential of $[Co((MeIm-Bpy)PF_6)_3]^{2+}$ is higher than both $[Co(dmb)_3]^{2+/3+}$ and I^-/I_3^- redox couples (Fig. 6). It could be probably due to the substitution of imidazolium cations which stabilize HOMO of the complex more than the bipyridine ligand. As for Fig. 6b, the higher redox potential of $[Co((MeIm-Bpy)PF_6)_3]^{2+/3+}$ redox couple reduce the excessive driving force for the dye regeneration reaction, due to the redox potential 1.08 V of N719 and therefore it is beneficial for improving the V_{oc} of the devices. Using dye N719, the overall power conversion efficiencies of 7.37% and 8.29% were attained at 100 and 50 mW cm^{-2} in a binary ionic liquid-based electrolyte under 1.5 solar spectrum illumination, respectively. These values are higher than those of pure I^-/I_3^- redox mediator under the same irradiation conditions. Moreover, after 800 h of testing, it was observed that the devices containing this new electrolyte retained around 76% of their initial conversion efficiency.

The relationship between the performance of DSSCs utilizing $[Co(bpy)_3]^{2+/3+}$ redox system and the carbazole dye structure was investigated by varying the bulkiness of the donor group and linker group.[67] The results showed that there is a constructive relationship between V_{oc} and the number of n-hexylthiophene units, bulkiness of the appendage group in the donor segment, and shorter alkyl chains in the thiophene linker moiety. Retardation of charge recombination increased the V_{oc}, indicating that longer and larger molecules exert better blocking function. Also, a series of efficient carbazole based sensitizers, JM1-JM3[76] and JK-318-JK320[77] were tested for DSSCs in the presence of Co-based redox mediators.
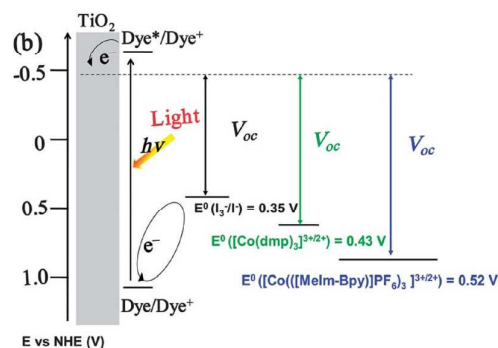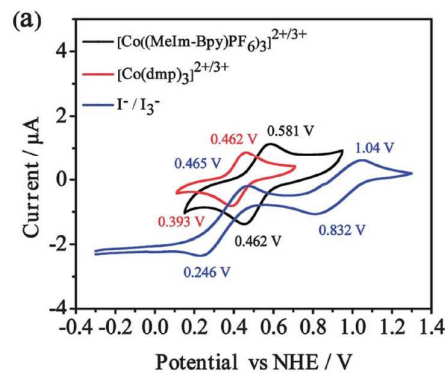
Fig. 6 (a) Cyclic voltammograms of 1.5 mM solutions of $[Co((MeIm-Bpy)PF_6)_3](PF_6)_2$ (black wave), $[Co(dmp)_3](PF_6)_2$ (red wave) and I^- (blue wave) in acetonitrile solution. (b) Schematic energy diagram for the DSSCs sensitized with the dye N719. Reproduced with permission from ref. 66. Copyright 2013, Royal Society of Chemistry.

In addition, one-dimensional ZnO nanowire (1D ZnO NW) and a metal-free, D-π-A type, carbazole dye (SK1) sensitizer-based photovoltaic device with a power conversion efficiency of more than 5% have been demonstrated by employing $[Co(bpy)_3]^{2+/3+}$ as redox shuttle.[70] In contrast, the identical DSSC with traditional I^-/I_3^- showed a η value of ∼ 4.7%. Recently, it was shown that 1D-ZnO based DSSCs using the homoleptic Ruthenium(II) dipyridophenazine complex as a photosensitizer employ cobalt complexes as the redox mediators.[83] The ZnO NW based DSSCs afforded a higher η value of ∼ 5.9% and ∼ 5.6% employing $[Co(bpy)_3]^{2+/3+}$ and $[Co(phen)_3]^{2+/3+}$ complexes, respectively.

For the first time, Xiang and coworkers reported the application of $[Co(bpy)_3]^{2+/3+}$ redox couple in an aqueous DSSC electrolytes in conjunction with a donor-π-acceptor dye.[84] Adjusting the concentration of polyethylene glycol in the aqueous electrolyte causes an improvement in short circuit current. It can be attributed to the better diffusion of the redox mediator within the electrolyte. Additionally, replacement of platinum counter electrodes with ITO/Pt composite as counter electrodes, increased energy conversion efficiency up to above 5%. Significantly, the photovoltaic parameters showed that $[Co(bpy)_3]^{2+/3+}$-based devices are more stable than $[Fe(CN)_6]^{4-/3-}$-based DSSCs[85] under illumination. Their efficiencies drop by more than 50% within the first 10 minutes of the illumination. Most importantly, the cobalt aqueous electrolyte-based device efficiencies decrease by only 10% over the initial 30 days of testing and then remains relatively constant over the following 60 days (Fig. 7).[84]
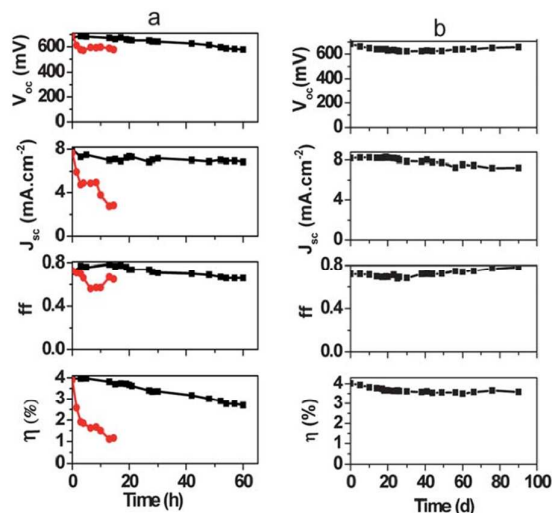
Fig. 7 Stability testing of aqueous DSSCs (a) under 100 mW cm2 white LED illumination; (b) in the dark (black: cobalt based device, red: hexacyanoferrate based device). Reproduced with permission from ref. 84. Copyright 2013, Royal Society of Chemistry.

N-doped hollow core-mesoporous shell carbon (N-HCMSC) capsules with high surface area was used as an efficient and alternative metal-free counter electrode for DSSCs. Applying Y123 dye and $[Co(bpy)_3]^{2+/3+}$ redox system, it showed η and FF values up to 8.76 and 77.6%, respectively.[86]

A relatively simple series of cyclometalated ruthenium dyes were applied in DSSCs using $[Co(dmb)_3]^{2+/3+}$ as mediator, which an overall power conversion efficiency of over 3% was achieved.[68]

It is shown that the post treatment of the dyed photoanodes with commercially available short chain tri-alkoxy propyl silanes bearing a positive charge may demonstrate a viable successful general strategy for improving the electron collection efficiency in cobalt mediated DSSCs. This observation happened even without use of highly sterically hindered dyes specifically designed to work in conjunction with kinetically fast metal based mediators.[87]

To examine the relationship between donor type in an organic dye and the recombination in DSSCs, various organic dyes were investigated in conjugation with $[Co(bpy)_3]^{2+/3+}$ redox couples.[69] These dyes comprise donor moieties including carbazole (MK-1), coumarin (MK-31), triphenylamine (MK-88) and N-phenyl-carbazole (MK-90). The highest V_{oc} and the longest electron lifetime were obtained with MK-88, which was attributed to the blocking effect by steric hindrance of the donor nonplanar structure. On the other hand, the lowest V_{oc} and shortest electron lifetime were attained via MK-31, proposing that coumarin attract the cobalt redox shuttles to the surface of the TiO_2 layer. This leads to an increase in the concentration of cobalt complex.

Cong et al. investigated a new TEMPO (2,2,6,6-tetramethyl-1-piperidinyloxy)-Co tandem redox system with $TEMPO^{0/+}$ and $[Co(bpy)_3]^{2+/3+}$ for DSSCs.[74] A large increase of 862 to 965 mV in V_{oc}, was detected in the new tandem redox system while the I_{sc} was essentially maintained. The conversion efficiencies of 7.1% and 8.4% were obtained for cells containing single $[Co(bpy)_3]^{2+/3+}$ redox couple and TEMPO-Co tandem redox system, respectively. LEG4 was used as sensitizer in these cases. Improving V_{oc} and the overall efficiency was ascribed to the partial regeneration of the sensitizing dye molecules by TEMPO. Using new redox system, the problem of faster recombination of the single TEMPO redox couple was resolved and the mass-transport of the metal-complex-based electrolyte was also improved. In addition, this TEMPO-Co tandem system has avoided the corrosive effects of iodine in the electrolyte

as well as showing a much higher V_{oc} and conversion efficiency. This result shows the better performance of TEMPO-Co tandem system rather than the single redox electrolyte systems based on Co. As seen in Fig. 8 the electron transfer processes can be formalized in the form of two cycles of redox exchange reactions. The first one is the single-component $Co^{2+/3+}$ redox cycle, and the second is the synergistic $TEMPO^{0/+}$-Co(II/III) cycle. So, a hoping future could be imagined for tandem systems instead of single redox shuttles in electrolytes for DSSCs.

YA422 is a typical organic sensitizer with indoline-based Hagfeldt-type donor. As a matter of fact, "Hagfeldt"-type donors based on indoline and triphenylamine are widely used to construct D-π-A organic sensitizers for DSSCs with cobalt redox shuttles. Hence, the overall efficiency of 10.65% was attained through dye YA422 with $[Co(bpy)_3]^{2+/3+}$ redox electrolyte based on single organic sensitizer.[75] In addition, two new pyrido[3,4-b]-pyrazine-based sensitizers with different cores of bulky donors including indoline for DT-1 and triphenylamine for DT-2, were investigated with cobalt electrolytes.[1] The strongly electron-withdrawing pyrido[3,4-b]pyrazine-based auxiliary acceptor was discovered to extend the absorption wavelength range and increasing I_{sc} of DSSCs compared to dye YA422. The photoelectric conversion efficiency of 8.57% was obtained by DSSCs based on DT-1 with cobalt redox electrolyte under standard AM 1.5 G simulated sunlight.

More recently, the performance of back-illuminated DSSCs with a $[Co(bpy)_3]^{2+/3+}$ redox couple and the organic dye MK-2 was considered as a replacement for I^-/I_3^- redox electrolyte and organic metallic dye N719.[88] Using thin TiO_2 films together with the naturally formed blocking layer at the outermost surface of Ti substrate, successfully alleviate the drawbacks of cobalt mediator. By virtue of these simultaneous effects, it attained a highly promising power conversion efficiency of 7.12%. This suggests that the cobalt redox complex is a particularly promising alternative redox mediator for back-illuminated DSSCs.

Photovoltaic parameters and the corresponding dyes for DSSCs based on Co redox shuttles are summarized in Table 1, 2 and 3 to provide a clear overall sense of the literature.
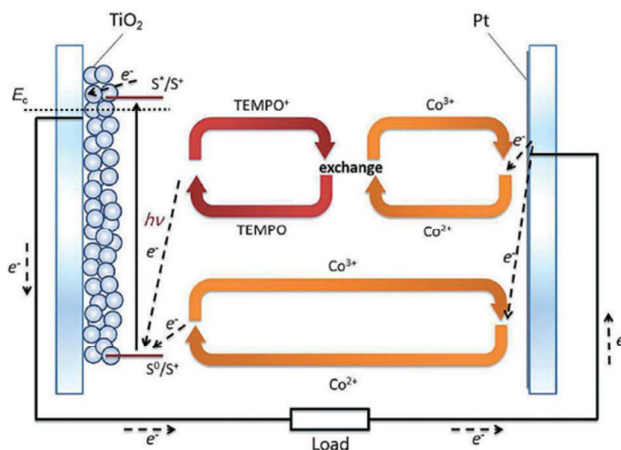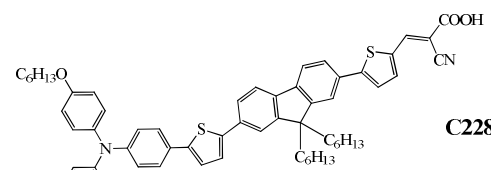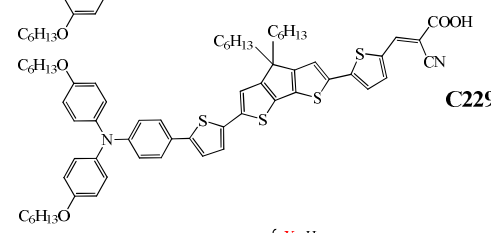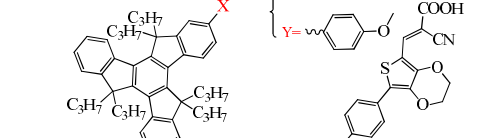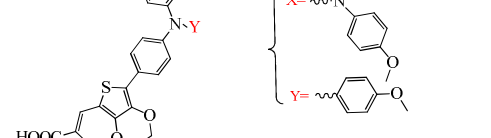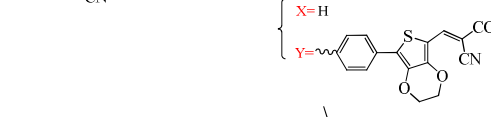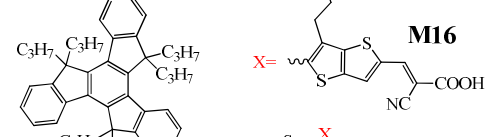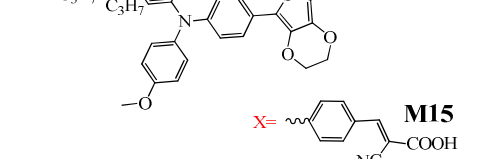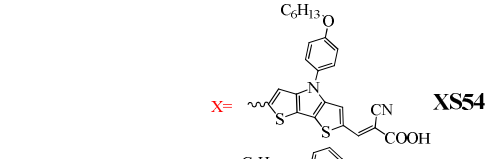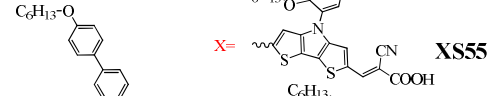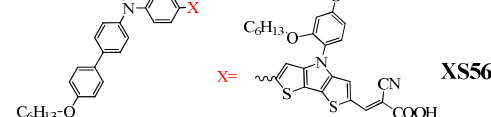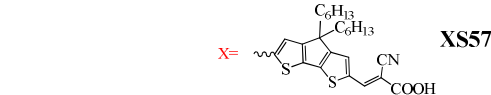
Fig. 8 Schematic description of the expected electron transfer processes in the TEMPO–Co tandem redox electrolyte. Reproduced with permission from ref. 74. Copyright 2014, Royal Society of Chemistry.

2.2 Co-phenanthroline-based mediators

Due to the limited electron diffusion length found for the cobalt complexes, Wang group employed different organic sensitizers based on $[Co(phen)_3]^{2+/3+}$ redox shuttle in combination with

Table 2 Photovoltaic parameters for DSSCs based on Co-phenanthroline mediators in combination with different dyes. For comparison the corresponding parameters for DSSCs containing the standard I^-/I_3^- redox couple are also reported, when available.

$[Co(phen)_3]^{2+/3+}$

phen= 1,10-phenanthroline

$[Co(Cl\text{-}phen)_3]^{3+/2+}$

Cl-phen= 5-chloro-1,10-phenanthroline

Electrolyte	Sensitizer	V_{oc} (V)	I_{sc} (mA cm^{-2})	FF	IPCE (%)	η (%)	Ref.
$[Co(phen)_3]^{2+/3+}$	C213	0.94	9.51	0.73	-	6.5	
	C230	0.90	10.72	0.73	-	7.1	
	C218	0.86	13.26	0.75	-	8.6	
							89
	C231	0.77	10.07	0.74	-	5.8	
	C232	0.79	10.68	0.75	-	6.3	
	C233	0.81	12.24	0.77	-	7.7	
$[Co(phen)_3]^{2+/3+}$ I^-/I_3^-	T1	0.82	7.99	0.76	-	5.0	
		0.8	7.78	0.75	-	4.6	
							90
$[Co(phen)_3]^{2+/3+}$ I^-/I_3^-	T3	0.84	12.98	0.74	-	8.0	
		0.75	12.86	0.71	-	6.9	
$[Co(phen)_3]^{2+/3+}$	C218	0.95	13.30	0.74	-	9.3	
	C244	0.95	10.54	0.77	-	7.7	
							91
	C245	0.93	12.05	0.75	-	8.4	
	C246	0.87	11.41	0.77	-	7.6	

Journal Name

Electrolyte	Dye	V_{oc}	J_{sc}	FF		η	Ref
$[Co(phen)_3]^{2+/3+}$ I^-/I_3^-	C228	0.83 / 0.76	7.60 / 7.78	0.74 / 0.74	- / -	4.7 / 4.4	
$[Co(phen)_3]^{2+/3+}$ I^-/I_3^-	C229	0.85 / 0.68	15.31 / 15.20	0.73 / 0.65	- / -	9.4 / 6.7	92
$[Co(phen)_3]^{2+/3+}$ I^-/I_3^-	M14	0.83 / 0.78	12.0 / 11.2	0.72 / 0.69	85 / -	7.2 / 6.0	
$[Co(phen)_3]^{2+/3+}$ I^-/I_3^-	M18	0.87 / 0.77	9.0 / 9.3	0.71 / 0.68	- / -	5.5 / 4.9	93
$[Co(phen)_3]^{2+/3+}$ I^-/I_3^-	M19	0.87 / 0.74	11.2 / 11.4	0.71 / 0.68	- / -	6.9 / 5.7	
$[Co(phen)_3]^{2+/3+}$ I^-/I_3^-	M16	0.90 / 0.68	11.9 / 12.2	0.71 / 0.68	- / -	7.6 / 5.6	94
$[Co(phen)_3]^{2+/3+}$ I^-/I_3^-	M15	0.87 / 0.76	9.6 / 11.8	0.70 / 0.68	- / -	5.8 / 6.1	
	XS54	0.85	13.5	0.71	-	8.14	
$[Co(phen)_3]^{2+/3+}$	XS55	0.95	11.2	0.70	-	7.45	95
	XS56	0.94	11.6	0.69	-	7.48	
	XS57	0.91	12.1	0.70	-	7.68	

RSC Advances Accepted Manuscript

Electrolyte	Dye structure	Dye	V_{oc}	J_{sc}	FF		η	Ref
$[Co(Cl\text{-}phen)_3]^{2+/3+}$	(ADEKA-1 structure) X= ADEKA-1	ADEKA-1	1.04	15.6	0.77	85	12.5	96
	X= ADEKA-2	ADEKA-2	-	-	-	-	-	
$[Co(phen)_3]^{2+/3+}/[Co(Etpy)_2]^{2+/3+}$ (EtPy= 4'-(2,3-dihydrothieno[3,4-b][1,4]dioxin-5-yl)-2,2':6',2"-terpyridine)		D35	0.92	8.4	0.67	-	5.1	97
$[Co(phen)_3]^{2+/3+}$	(M36/M37 structure) X= M36	M36	0.93	15.01	0.69	-	9.58	98
	X= M37	M37	0.68	11.03	0.83	-	6.19	
$[Co(phen)_3]^{2+/3+}$ I^-/I_3^-	(XS51 structure)	XS51	862 / 0.75	10.5 / 11.6	0.65 / 0.67	78.7 / 80.6	5.88 / 5.68	99
$[Co(phen)_3]^{2+/3+}$ I^-/I_3^-	(XS52 structure)	XS52	830 / 0.74	11.5 / 12.0	0.68 / 0.69	- / -	6.58 / 6.13	

relatively thin TiO$_2$ films of about 6 to 7 μm. They attained the overall power conversion efficiencies of 7.1%, 7.7%, 8.0% and 8.4% with C230[89], C233[89], T3[90] and C245[91] dyes, respectively. Even higher efficiencies were achieved using C218 dye[100] (9.3%)[91] as well as the C229 (9.4%), showing a significant red shift at the absorption edge[92].

However, the optimization of DSSCs sensitized with M14 in combination with a $[Co(phen)_3]^{2+/3+}$ redox electrolyte yield a DSSC with an overall power conversion efficiency of 7.2% under AM 1.5 irradiation (100 mW cm^{-2}).[93] The hexapropyltruxene unit retards the rate of interfacial back electron transfer from the conduction band of TiO$_2$ film to the oxidized electrolyte. This process enables the ability of high photovoltages approaching to 0.9 V. Also, the better efficiency was obtained with the truxene–based organic dye (M16)-sensitized device and $[Co(phen)_3]^{2+/3+}$ which displays an efficiency of 7.6% at standard conditions. Additionally, the studies of recombination kinetics of Co(III) complexes at titania/dye interface with D-π-A organic dyes including M36 and M37, showed that a Marcus inverted region can be reached for the charge recombination kinetics behavior of Co(III) species for M36 sensitized DSSCs.[98] Benefiting from a Marcus inverted region behavior, the M36 dye displayed a good compatibility with the $[Co(phen)_3]^{2+/3+}$ redox couples.

Dithieno[3,2-b:2',3'-d]pyrrole (DTP)-based triphenylamine sensitizers (XS54-XS57) with different hexyloxyphenyl (HOP) substituents were synthesized and applied in DSSCs along with $[Co(phen)_3]^{2+/3+}$ redox shuttle.[95] XS54 featuring the 4-HOP-DTP spacer, yield a η of 8.14% in combination with the cobalt electrolyte. Additionally, the photovoltaic performances of $[Co(phen)_3]^{2+/3+}$ redox couple were superior to those of I$^-$/I$_3^-$ redox couple for TiO$_2$ film DSSCs which sensitized by XS51-XS52. This represents that the rational design of sterically bulky organic dyes is needed for further progress of high-efficiency iodine-free devices.[99]

DSSCs constructed via a novel metal-free alkoxysilyl carbazole as a sensitizing dye and a Co(II/III)-complex redox electrolyte showed an overall efficiency of over 12% with V$_{oc}$ higher than 1 V by applying a hierarchical multi-capping treatment to the photoanode.[96] This dye was used with two Co-based mediators including $[Co(Cl\text{-}phen)_3]^{2+/3+}$ (Table 2) and $[Co(bpy)_3]^{2+/3+}$. The higher V$_{oc}$ value was obtained via the former one, which has a redox potential of 0.72 V vs. NHE in the ADEKA-1-sensitized cell.

A mixture of $[Co(phen)_3]^{2+/3+}$ and $[Co(EtPy)_2]^{2+/3+}$ complexes, was utilized as redox mediator in DSSCs, where EtPy is a terpyridine ligand bearing 3,4-ethylenedioxythiophene (EDOT) substituent.[97] $[Co(EtPy)_2]^{2+}$ complex acts as co-mediator in the presence of $[Co(phen)_3]^{2+}$. The low solubility of this complex prevents its individual applying. The addition of $[Co(EtPy)_2]^{2+}$ to $[Co(phen)_3]^{2+}$ provided an electron cascade which leads to an enhancement in cell efficiency. A synergy between the EDOT-functionalized cobalt complex and the PEDOT counter-electrode is responsible for this effect which favors electron transfer and reduces the recombination.

RSC Advances Accepted Manuscript

2.3 Other mediators of Co complexes

In 2001, for the first time, Nusbaumer et al. employed $[Co(dbbip)_2]^{2+}$ (dbbip= 2,6-bis(1'-butylbenzimidazol-2'-yl)pyridine) (Table 3), as redox shuttle in DSSCs, for explaining the effects of cobalt electrolyte on recombination process.[101] With this new one-electron redox shuttle, DSSCs sensitized by dye Z316 achieved an overall electrical power conversion efficiency of 2.2% under AM1.5 irradiation (100 mW cm^{-2}). The results showed that in the absence of Co(II/III) redox couple, the absorption signal was decreased as a result of increase in dynamic recombination process between oxidized dye and the conduction band of the semiconductor.[101] In addition, this group reported a series of cobalt complexes used as redox shuttles in electrolytes of DSSCs.[102] Among the compounds investigated, $[Co(dbbip)_2]^{2+/3+}$ showed the highest efficiency of 4.2% together with a ruthenium-based dye, Z907. Through screening the redox couple, they demonstrated a relationship between the redox potential and V_{oc}, in a way that V_{oc} increases with $E_{1/2}$. Furthermore, their results showed the influence of sensitizer structure on the behavior of the cobalt redox couple. An explanation for this observation is that when the dye is less sterically hindered, there is a possibility of forming an ion-pair with the Co(III). This means the reduction in diffusion rate of Co(III) that can affect the overall photocurrent negatively.[102] The electrochemical properties of the redox mediator $[Co(dbbip)_2]^{2+/3+}$ were also studied in a mixed acetonitrile/ethylene carbonate solvent by a range of techniques in order to determine the rate constants for electron transfer and the diffusion coefficients of Co(II) and Co(III) species.[103]

Wang and co-workers indicated that the electron diffusion length in DSSCs is substantially reduced when the conventional I^-/I_3^- electrolyte is replaced by $[Co(dbbip)_2]^{2+}$ redox shuttle complex.[104]

Nevertheless, optimization of the cell efficiencies also requires the optimization of the counter electrode/electrolyte interface. Thus, in order to improve the efficiency, an FTO-supported graphene nanoplatelet cathode (GNP-FTO) was applied in DSSCs based on Co-bipyridine-pyrazole redox couple. The exchange currents for $[Co(L)_2]^{2+/3+}$ (L= 6-(1H-pyrazol-1-yl)-2,2'-bipyridine) couple on the GNP-electrode scaled linearly with the GNP films optical absorbance, and they were by 1-2 orders of magnitude larger than those for the I^-/I_3^- couple on the same electrode. DSSCs with Y123 dye adsorbed on TiO$_2$ photoanode reached energy conversion efficiencies between 8 and 10% for both GNP and Pt-based cathodes.[105]

Moreover, $[Co(bpy-pz)_2]^{2+/3+}$ complex using tridentate ligands adsorbed on TiO$_2$ as a redox mediator in combination with Y123 dye. This combination yielded a power conversion efficiency of over 10% at 100 mW cm^{-2}.[24] A device kept at ambient conditions showed no loss in the conversion efficiency after 1 month, which is a promising result. This result shows that the molecularly engineered cobalt redox couple is a legitimate alternative to the commonly used I^-/I_3^- redox shuttle. Recently, a peak power conversion efficiency of 10.6% was achieved under full sun light intensity through employing the same mediator and dye, and modifying fluorine-doped tin-oxide with using a thin and conformal TiO$_2$ blocking layer by ALD technique.[106]

A series of cobalt complexes with various polypyridyl ligands containing electron acceptor groups on pyridyl or pyrazole, were used as one-electron redox mediators in DSSCs together with polymer based cathode resulting in an excellent performance.[107] The performance of DSSCs using the molecularly engineered cobalt redox couple and poly(3,4-alkylthiophenes) based cathode was better than the I^-/I_3^- redox shuttle with platinized cathode and the efficiencies increased from 1.61 to 10.24% at 0.1 sun irradiation.

The application of a new class of redox mediators based on $[Co(PY5Me_2)(MeCN)]^{2+/3+}$ complex (Table 3) was reported by Kashif et al. (where PY5Me$_2$ is the pentadentate ligand, 2,6-bis(1,1-bis(2-pyridyl)ethyl)pyridine).[108] By X-ray crystallography, it is shown that the MeCN ligand can be replaced by more strongly coordinating Lewis bases (B) to give complexes with the general formula of $[Co(PY5Me_2)(B)]^{2+/3+}$, where B= 4-TBP or N-methylbenzimidazole (NMBI). Thus, applying a pentadentate ligand allows not only the potential of the Co(II/III) redox couple to be tuned through the single-site coordination, but also expects to result in a lower re-organizational energy for electron transfer in comparison to the $[Co(bpy)_3]^{2+/3+}$ redox couple. Curves I-V show the best performing DSSCs for each redox couple (Fig. 9). The lower I_{sc} values for $[Co(PY5Me_2)(TBP)]^{2+/3+}$ could be a consequence of less efficient dye-regeneration, and may arise from the lower driving force for this reaction (0.24 V). Also, for devices based on $[Co(PY5Me_2)(NMBI)]^{2+/3+}$ the mass-transport limitations compared to $[Co(bpy)_3]^{2+/3+}$ was found. Employment of the electrolytes based on $[Co(PY5Me_2)(NMBI)]^{2+/3+}$ complex in combination with a strongly absorbing organic dye, MK2, yielded devices with efficiencies of 9.2% and 8.4% at 0.1 and 1 sun irradiation, respectively. These values are higher than the analogous devices applying the $[Co(bpy)_3]^{2+/3+}$ redox couple. In addition, V_{oc} of almost 1.0 V at 100% sun was measured for devices fabricated with the TBP complex.[108]

Moreover, stable DSSC electrolytes based on Co(II/III) complexes of a hexadentate pyridine ligand ((6,6'-bis(1,1-di(pyridin-2-yl)ethyl)-2,2'-bipyridine, bpyPY4) was reported by the same group.[109] The devices fabricated with these mediators were found to outperform the prototypical $[Co(bpy)_3]^{2+/3+}$ redox mediator both in terms of the overall efficiency and stability under full sun irradiation conditions. An impressive efficiency of 8.3% was attained for the DSSCs based on this the new redox couple. DSSCs based on this electrolyte outperformed those assembled with the reference mediator Co-bpy, showing a > 20% performance increase over the first 24 h of continuous illumination (Fig. 10). With TFMP (p-trifluoromethylpyridine), the DSSCs based on $[Co(bpyPY4)]^{2+/3+}$ presented a 20% increase in performance, which maintained across the full 100 h testing period. In the case of NMBI, the DSSCs exhibited the same initial improvement in performance but there was a gradual decrease and stabilization at about 90% of the original value after 100 h testing.[109]
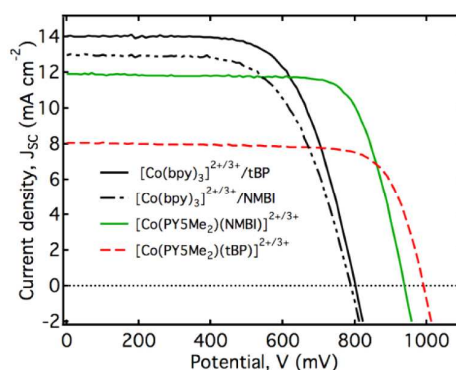
Fig. 9 Comparison of DSSC performance for optimized devices sensitized with MK2 based on $[Co(PY5Me_2)(NMBI)]^{2+/3+}$ (green line), $[Co(PY5Me_2)(TBP)]^{2+/3+}$ (red dashed), $[Co(bpy)_3]^{2+/3+}$/TBP (black solid), and $[Co(bpy)_3]^{2+/3+}$/NMBI (black dotted) electrolytes in acetonitrile, measured at AM1.5 G; 1000 W m^{-2}. Reproduced with permission from ref. 108. Copyright 2012, American Chemical Society.

Table 3 Photovoltaic parameters for DSSCs based on mediators of Co in combination with different dyes. For comparison the corresponding parameters for DSSCs containing the standard I⁻/I₃⁻ redox couple are also reported, when available.

$[Co(bpy\text{-}pz)_2]^{2+/3+}$ $[Co(ttcn)_2]^{2+/3+}$ $[Co(en)_3]^{2+/3+}$

X=H $[Co(terpy)_2]^{2+/3+}$
X=Cl $[Co(Cl\text{-}terpy)_2]^{2+/3+}$

X= butyl $[Co(dbbip)_2]^{2+/3+}$
X= methyl $[Co(dmbip)_2]^{2+/3+}$

$[Co(abpn)]^{0/1+}$

x= $[Co(PY5Me_2)(TBP)]^{2+/3+}$
x= $[Co(PY5Me_2)(NMBI)]^{2+/3}$

$[Co(bpyPY4)]^{2+/3+}$ $[Co(py\text{-}pz)_3]^{2+/3+}$

$[Co(py\text{-}pzMe_2)_3]^{2+/3+}$ $[Co(sep)]^{2+/3+}$

Electrolyte	Sensitizer	V_{oc} (V)	I_{sc} (mA cm^{-2})	FF	IPCE (%)	η (%)	Ref.
$[Co(dbbip)_2]^{2+/3+}$	**Z316**	0.67	6.8	0.46	65	2.2	[101]
$[Co(dbbip)_2]^{2+/3+}$	**Z907**	0.66	6.5	0.76	38	4.2	[102]
$[Co(dmbip)_2]^{2+/3+}$		0.65	4.2	0.76	25	2.7	
$[Co(terpy)_2]^{2+/3+}$		0.47	1.4	0.70	11	0.5	
$[Co(bpy\text{-}pz)_2]^{2+/3+}$ (Pt cathode)	**Y123**	0.98	1.37	0.74		10.0	[105]
$[Co(bpy\text{-}pz)_2]^{2+/3+}$ (graphene cathode)		0.96	1.34	0.76		9.7	
$[Co(bpy\text{-}pz)_2]^{2+/3+}$	**Y123**	0.93	1.23	0.77	-	9.30	[24]
I⁻/I₃⁻		0.71	1.27	0.74	-	7.03	
$[Co(PY5Me_2)(NMBI)]^{2+/3}$	**MK2**	0.94	11.8	0.77		8.4	[108]
$[Co(PY5Me_2)(TBP)]^{2+/3}$		0.99	8.1	0.76		6.1	
$[Co(py\text{-}pz)_3]^{2+/3+}$	**Y123**	0.87	1.0	0.76		7.15	[107]
$[Co(py\text{-}pzMe_2)_3]^{2+/3+}$		0.8	0.96	0.19		1.61	
$[Co(Cl_2bpy)_3]^{2+/3+}$		0.84	1.3	0.66		7.63	
$[Co(ttcn)_2]^{2+/3+}$	**MK2**	-	-	-	-	2	[26]

$[Co(sep)]^{2+/3+}$		-	-	-	-	1.4×10^{-5}	110
I^-/I_3^-		-	-	-	-	3.8×10^{-4}	
$[Co(en)_3]^{2+/3+}$	**PMI-6T-TPA**	0.71	4.44	0.42	-	1.30	111
$[Co(bpyPY4)]^{2+/3+}$	**MK-2**	0.76	14.7	0.75	-	8.30	109
$[Co(Cl\text{-}terpy)_2]^{2+/3+}$	**Y123**	0.92	13.7	0.68	-	8.7	9
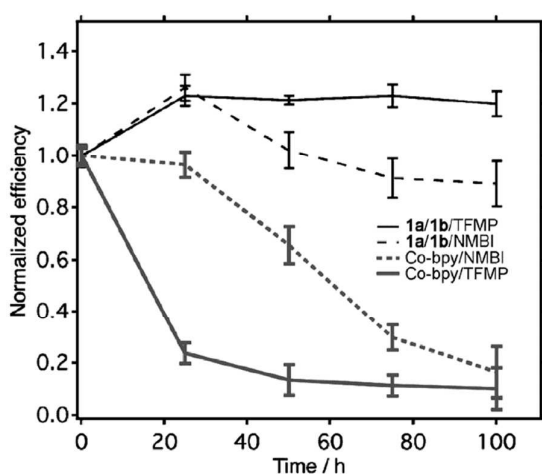
Fig. 10 Normalized efficiencies of the devices under full sun irradiation aging experiment is shown with a 400 nm UV-cut off filter. Two Lewis bases, NMBI and TFMP, were alternatively used with 1a/1b and Co-bpy (4:1, MeCN:VN). Reproduced with permission from ref. 109. Copyright 2013, Wiley-VCH Verlag GmbH & Co. KGaA, Weinheim.

A new low-spin cobalt(II) complex, $[Co(ttcn)_2]^{2+/3+}$ (ttcn= trithiacyclononane), was investigated as a redox shuttle for use in DSSCs.[26] This unique redox shuttle is stable, transparent and easy to synthesize from commercial ligands. It has also attractive energetic and kinetic features for use in DSSCs. Moreover, the formal potential of $[Co(ttcn)_2]^{2+/3+}$ is 0.69 V versus NHE, which is ~ 60 mV positive than $[Co(bpy)_3]^{2+/3+}$. So, it potentially permits fairly greater photovoltages. Initial results showed that the overall performance of dye N719 is restricted by recombination, due to the more positive potential and larger self-exchange rate constant of $[Co(ttcn)_2]^{2+/3+}$ compared to that of $[Co(bpy)_3]^{2+/3+}$. However, the better performance was obtained with Z907 sensitizer and deposition of an ultrathin alumina coating on nanoparticle-based TiO_2 DSSC photoanodes. The performance of MK-2 dye is significantly improved in comparison with DSSCs employing Z907, with an efficiency of over 2% achieved for the $[Co(ttcn)_2]^{2+/3+}$/MK-2 system.[26]

It was reported that p-type DSSCs with $[Co(sep)]^{2+/3+}$ (Table 3), $[Co(bpy)_3]^{2+/3+}$, and I^-/I_3^- redox mediators benefit from a multilayer Zn(II) tetraphenylporphyrin chromophores, which is assembled through copper catalyzed azide-alkyne cycloaddition (CuAAC).[110] This is the first use of $[Co(sep)]^{2+/3+}$ as a redox mediator for DSSCs which provides an alternative cobalt-based redox mediator for p-type DSSCs with more negative reduction potential rather than $[Co(bpy)_3]^{2+/3+}$. However, the highest current densities were attained with I^-/I_3^- as the redox mediator while $[Co(sep)]^{2+/3+}$ generated the highest potentials. For all three electrolytes, I_{sc} was improved with the addition of porphyrin layers beyond a monolayer. The maximum power was achieved with a device containing three porphyrin layers and $[Co(bpy)_3]^{2+/3+}$ redox shuttle which resulted in an efficiency of 1.5×10^{-3} %.

Nevertheless, I_{sc} was reached a maximum value at a point superior than one layer after which it decreases. It could be probably due to exciton diffusion limitations and the insulating effects of the multilayer film.[110]

Applying tris(1,2-diaminoethane)cobalt(II/III) complexes ($[Co(en)_3]^{2+/3+}$) as redox mediators in p-DSSCs was reported with the redox potential of about 340 mV more negative than that of typical I^-/I_3^- based p-DSSC electrolytes.[111] It offers the scope to dramatically increase the V_{oc} of p-DSSCs. The $[Co(en)_3]^{2+/3+}$ electrolytes are optically transparent, making them suitable for use in tandem solar cells. Photocathodes based on this mediator produced the highest V_{oc} of 709 mV with an efficiency of 1.3%.

Moreover, cobalt-bis-2,2',6',2''-terpyridine complexes allow systematic tuning of the redox potential by variation of the substituents on the terpyridine ligand. This ultimately improves the open circuit voltage and the efficiency of the device. Two cobalt terpyridine complexes including $[Co(terpy)_2](B(CN)_4)_{2/3}$ and $[Co(Cl\text{-}terpy)_2](TFSI)_{2/3}$ as redox electrolytes, displayed the importance of the ligand substitution . It determines the dark current and V_{oc} values of the device due to tuning of the electrolyte energy level. The redox potential of $[Co(Cl\text{-}terpy)_2](TFSI)_2$ mediator is 130 mV more positive than $[Co(terpy)_2](B(CN)_4)_2$ mediator. $[Co(Cl\text{-}terpy)_2](TFSI)_{2/3}$ based electrolyte in combination with Y123 dye yielded an overall η of 8.7% under standard condition with V_{oc} values of over 900 mV.[9]

3. Fe-based redox mediators

Iron (Fe) is the most common and economical element in comparison with other metals on the earth. Table 4 shows the structures of Fe complexes as redox shuttles used in DSSC together with the corresponding photovoltaic parameters. Among Fe compounds, ferrocenium/ferrocene couple has great advantages as a redox system with respect to the remarkable electrochemical properties. However, one-electron redox couples also indicate enhanced recombination with photoinjected electrons. Therefore, the methods are needed to inhibit this recombination for functioning DSSCs, which eliminates the photovoltaic effect. [112] A study of the interfacial recombination processes in DSSCs has been done by Gregg and co-workers which introduce two techniques for passivating these interfaces in order to decreasing the recombination loss rates.[32] These methods lead to a marked decrease in the rate of interfacial charge recombination because of creating an electrochemical overpotential for the recombination process. Therefore, they allow employment of kinetically fast redox shuttles in DSSCs.[32] In 2010, Feldt et al. passivated dye-sensitized TiO_2 surfaces by a CH_3SiCl_3 reaction in order to decrease the fast recombination rates when using the ferrocene redox couple.[112] The insulating poly(methylsiloxane) film on the dye-sensitized TiO_2 surface acts as an efficient barrier for interfacial electron-transfer processes (photoinjected electrons with ferrocenium). Thus, the efficiency of the DSSC will be improved. The significant efficiency was obtained after two cycles of silane treatment for both N719 (0.36%) and Ru(bpy)$_2$(dcbpy) (0.51%) as sensitizers.[112]

Moreover, atomic layer deposition as a useful method was used to create conformal TiO_2 blocking layers on FTO substrates in DSSCs, effectively eliminating shunting.[113,114] These modified electrodes allow Fc/Fc$^+$, an outer-sphere redox couple, to be used as an electrolyte. The results showed that the addition of a blocking layer can dramatically improve the photovoltaic performance. These counteractions display interesting effects on the DSSC efficiency, but the resulting devices did not show high efficiencies (η < 0.4%).

An energy conversion efficiencies of 7.5% for DSSCs combining the archetypal ferrocene/ferrocenium (Fc/Fc$^+$) single-electron redox couple with a novel metal-free organic donor–acceptor sensitizer (Carbz-PAHTDTT) was reported by Daeneke et al.[8] Under the same conditions, these Fc/Fc$^+$-based devices exceed the efficiency achieved for I$^-$/I$_3^-$ electrolyte. This reveals the great potential of ferrocene-based mediators in future DSSCs applications and more favorable matching of the redox potential with that of the dye. Moreover, they reported a series of ferrocene derivatives that their redox potentials cover a wide range (0.09–0.94 V vs. NHE) by virtue of simple alkylation and halogenation of the cyclopentadienyl ring (Br$_2$Fc$^{0/+}$, BrFc$^{0/+}$, EtFc$^{0/+}$, Et$_2$Fc$^{0/+}$ and Me$_{10}$Fc$^{0/+}$).[115] The same solar conversion efficiencies of 4.3–5.2% and also IPCE results were attained using Fc, Et$_2$Fc and EtFc. The BrFc and Br$_2$Fc displayed lower energy conversion efficiencies than Et$_2$Fc, EtFc and Fc even with their more favorable redox potentials. In addition, their results indicated that Et$_2$Fc, EtFc and Fc, promote fast dye regeneration by providing the driving forces of 35-46 kJ mol^{-1}. However, this is not the case for BrFc and Br$_2$Fc, in which the driving forces are ≤ 18 kJ mol^{-1}. To improve the efficiency of Fc-based DSSCs, the ferrocene derivatives should also be matched to dyes with appropriate energy levels, such that ΔE= 0.36 V. Consequently, the halogen and alkylated ferrocene derivatives could be utilized in conjunction with dyes and panchromatic dyes showing higher and lower D/D$^+$ potentials, respectively.[115]

A Fc/Fc$^+$ redox couple was employed, as a model electrolyte, in quantum dot DSSCs.[116] Besides, a similar redox couple of prussianblue type nickel hexacyanoferrate redox mediator, K$_4$Ni^{II}[Fe^{II}(CN)$_6$]/K$_3$Ni^{II}[Fe^{III}(CN)$_6$], was used in solid state DSSCs.[117]
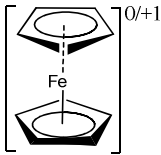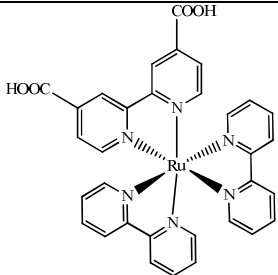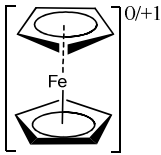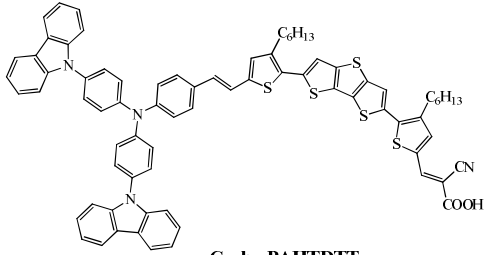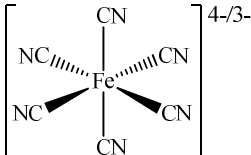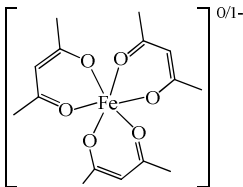
The current consensus is that water is an undesirable contaminant in DSSC electrolytes as it causes to the formation of iodate, dye desorption, low device efficiencies and device instability. However, Daeneke et al. exhibited that the carbazole dye, MK2, performs exceptionally well in DSSCs constructed with aqueous electrolytes, and the efficiencies of over 4% can be reached via applying [Fe(CN)$_6$]$^{4-/3-}$ redox couple.[85] The devices were found to demonstrate an increased stability when short wavelength light (< 480 nm) was omitted. It confirms the photocatalytic degradation of the redox couple as cause of the reduced device stability under white light illumination. However, the cyanide ligands might be replaced with stronger binding ligands, improving the stability. Fig. 11 shows a negligible efficiency drop of cobalt cell when it was left in ambient conditions for about three months.

In an interesting work, an efficient p-type DSSCs based on the readily available and inexpensive coordination complex tris(acetylacetonato)iron(III)/(II) ([Fe(acac)$_3$]$^{0/1}$) as redox mediator in conjunction with the PMI–6T–TPA sensitizer.[118] Despite a 170 mV more negative redox potential of [Fe(acac)$_3$]$^{0/1}$ compared to [Co(en)$_3$]$^{2+/3+}$, the V$_{oc}$ of [Fe(acac)$_3$]-p-DSSCs were lower than those measured for [Co(en)$_3$]-p-DSSCs. Nonetheless, the [Fe(acac)$_3$]-p-DSSCs displayed a higher IPCE (57%) than those based on [Co(en)$_3$]$^{2+/3+}$ and I$^-$/I$_3^-$ (Fig. 12). Measurement of the kinetics of dye regeneration by [Fe(acac)$_3$]$^{0/1}$ complex revealed that the process is diffusion limited, quantitative (> 99%), and about 50 times faster than measured for [Co(en)$_3$]$^{3+}$. Devices containing [Fe(acac)$_3$]$^{0/1}$ and a NiO blocking layer together with chenodeoxycholic acid as an electrolyte additive attained an efficiency of 2.51 %.
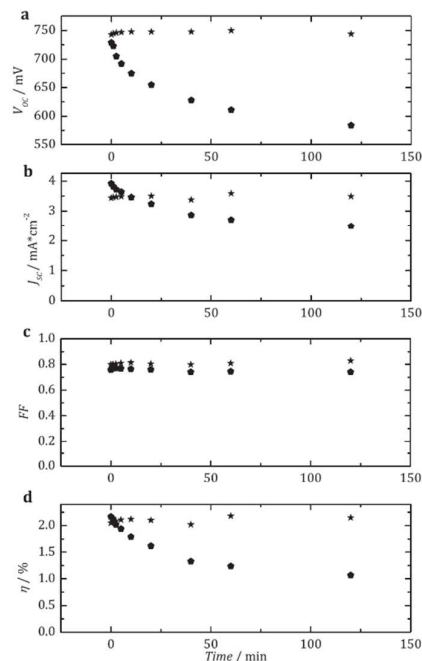
Fig. 11 Device stability of [Fe(CN)$_6$]$^{4-/3-}$ mediated devices during light soaking with green (stars) and blue (pentagons) light. The performance parameters a) V$_{oc}$ b) J$_{sc}$ c) FF and d) efficiency were measured at filtered (480 nm cut off) one sun AM 1.5 light. Reproduced with permission from ref. 85. Copyright 2012, Wiley-VCH Verlag GmbH & Co. KGaA, Weinheim.

Table 4 Photovoltaic parameters for DSSCs based on mediators of Fe in combination with different dyes.

Electrolyte	Sensitizer	V_{oc} (V)	I_{sc} (mA cm^{-2})	FF	IPCE (%)	η (%)	Ref.
[Fe] 0/+1		-	-	-	-	0.51	[112]
[Fe] 0/+1	Carbz-PAHTDTT	0.84	12.2	0.73	-	7.5	[8]
Me$_{10}$Fc	Carbz-PAHTDTT	0.35	1.36	0.48	79	2.2	[115]
Et$_2$Fc		0.48	1.34	0.64	77	4.0	
EtFc		0.54	1.34	0.69	79	4.9	
Fc		0.60	1.31	0.70	76	5.4	
BrFc		0.58	0.64	0.61	40	2.2	
Br$_2$Fc		0.52	0.52	0.58	30	1.5	
[Fe(CN)$_6$] 4-/3-	MK2	0.7	0.77	0.81	-	4.20	[85]
	Z907	0.59	0.15	0.71	-	0.62	
[Fe(acac)$_3$]$^{0/1-}$	PMI-6T-TPA	0.65	7.65	0.51	-	2.51	[118]
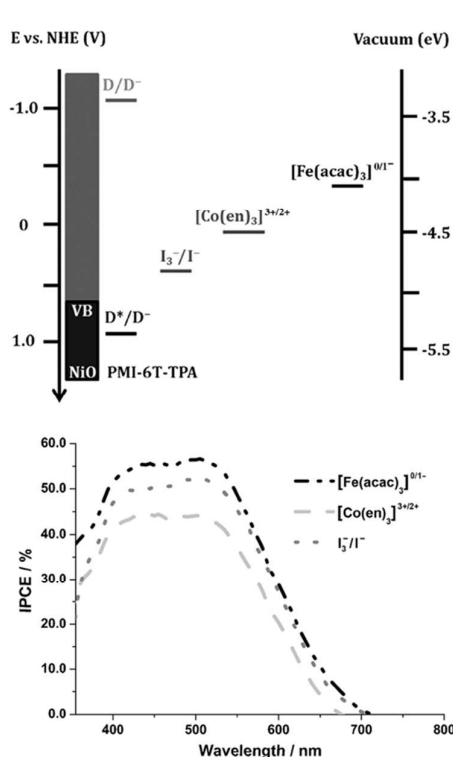
**Fig. 12** The energy-level diagram (top) and IPCE comparison (low) of I^-/I_3^-, $[Co(en)_3]^{2+/3+}$ and $[Fe(acac)_3]^{0/1-}$ electrolytes. Reproduced with permission from ref. 118. Copyright 2015, Wiley-VCH Verlag GmbH & Co. KGaA, Weinheim.

4. Cu-based redox mediators

For the first time, in 2005, a series of blue copper model complexes $(([Cu(SP)(mmt)]^{0/-}, [Cu(dmp)_2]^{2+/+}$ and $[Cu(phen)_2]^{2+/+})$ (Table 5) were examined for their effectiveness as redox shuttles in DSSCs by Yanagida and coworkers.[119] They afford a maximum IPCE of 40%, which is thought to stem from a slow regeneration of the N3 ruthenium photosensitizer owing to the large reorganization energies of copper(I/II) complexes.[120] The resulting electron self-exchange rate constant decreases in the order of: $[Cu(dmp)_2]^{2+/+}$ > $[Cu(SP)(mmt)]^{0/-}$ > $[Cu(phen)_2]^{2+/+}$. It is in agreement with the order of the smaller structural change between the copper(II) and copper(I) complexes due to the distorted tetragonal geometry. Under the weak solar light irradiation of 20 mW/cm^2 intensity, the maximum η value was obtained as 2.2% for DSSC using $[Cu(dmp)_2]^{2+/+}$. Whereas, a higher V_{oc} of the cell was attained compared to that of the conventional I^-/I_3^- couple.[119] The $[Cu(dmp)_2]^{2+/+}$ redox shuttle was employed in combination with a bilayer titania thin-film stained with a high-absorption-coefficient organic dye C218 which generates an impressive power conversion efficiency of 7.0%.[121] A broad 87% IPCE plateau of about 87% was observed in the spectral coverage from 460 to 580 nm for a typical cell with the iodine control electrolyte (Fig. 13). However, the copper redox shuttle displayed very low electron transfer rates on several noble metals, carbon black and conducting oxides, resulting in the poor fill factor.

A series of Cu(I/II) redox-shuttles-based on substituted bipyridines and pyridil-quinoline complexes were used as electron transfer mediators in regenerative photoelectrochemical cells (Table 5).[122] The best performing mediators attained maximum IPCEs of the order of 35–40%. The reasons of such low efficiencies could be explained by a slow dye reduction, leading to modest I_{sc}, rather than
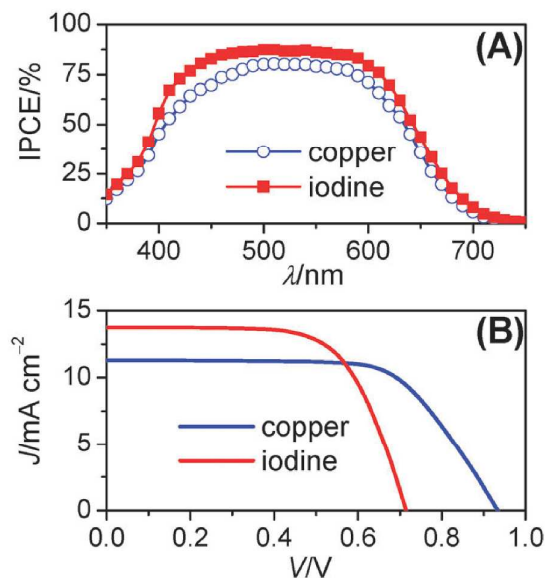
Fig. 13 (A) Photocurrent action spectra and (B) I–V characteristics under irradiation of 100 mW cm^{-2} simulated AM1.5G sunlight. Reproduced with permission from ref. 121. Copyright 2011, Royal Society of Chemistry.

by an efficient photoinjected electron/Cu(II) recombination, since both the V_{oc} and the FF obtained with copper mediated cell were higher than the corresponding I^-/I_3^--based DSSC.
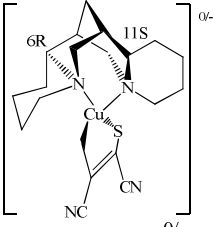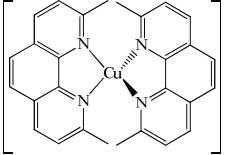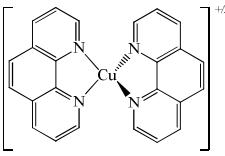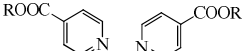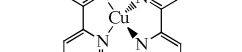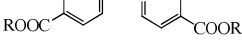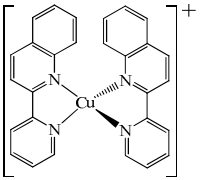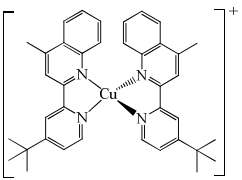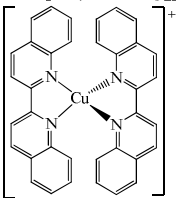
Yuan et al. reported two polyoxometalate (Anderson-type heteropolyanion) supported copper phenanthroline complexes, POM1-Cu-phen and POM2-Cu-phen, into DSSC electrolyte as the redox shuttles for achieving high solar energy conversion in DSSC.[123] The combination of Anderson-type heteropolyanions restrains the fast electron–hole recombination at the dyed TiO$_2$ photoelectrode/electrolyte interface, simplifies the electron transfer from Cu (I) to dye cation, and tunes the redox potential of $[Cu(phen)_2]^{+/2+}$ effectively. The V_{oc} values of the cells with POM1-Cu-phen, POM2-Cu-phen, and Cu-phen are consistent with the redox potential values and in the order: POM1-Cu-phen (472 mV) > POM2-Cu-phen (466 mV) > Cu-phen (372). In addition, under the same potential bias, the dark current for POM1/POM2-Cu-phen redox couples was strikingly smaller than that for the Cu-phen redox couple. The DSSCs based on both POM1/POM2-Cu-phen redox couples displayed higher I_{sc} and V_{oc} in comparison to the Cu-phen mediator, with the result that the performance of the Cu-phen redox couple DSSCs was improved about 4 times.

5. Ni, V and Os-based redox mediators

Nickel complexes of Ni(III/IV)bis(dicarbollide), were employed for the first time as an one-electron outersphere and non-corrosive redox shuttles in DSSCs.[31,124] In compared with Fc/Fc$^+$ shuttles, the $[Ni(carbollide)_2]^{-/0}$ (Fig. 14) system has many favorable properties, including fast dye regeneration, fast mass transport, and attractive electron transfer kinetics aspects. In Fig. 14, 3 and 4 species exhibit high thermal stability (up to 300 °C). An impressive improvement of the efficiency in DSSCs (1.5%) was observed through TiO$_2$ surface passivation via conformal, Å-precise atomic layer deposition (ALD) of Al$_2$O$_3$. In the same concentration, the regeneration was actually found to be faster than I^- and recombination was shown to be 1,000-fold slower than ferrocene. This could be attributed to the activation barrier of reducing Ni(IV) to Ni(III) which induces a cis-to-trans conformation change, making this reaction less prohibitive.[31]

Table 5 Photovoltaic parameters for DSSCs based on mediators of Cu in combination with different dyes.

Electrolyte	Sensitizer	V_{oc} (V)	I_{sc} (mA cm^{-2})	FF	IPCE (%)	η (%)	Ref.
[Cu(SP)(mmt)]$^{0/-}$	**N719**	0.66	4.4	0.44	-	1.3	[119]
[Cu(dmp)$_2$]$^{+/2+}$	**N719**	0.79	3.2	0.55	-	1.4	[119]
[Cu(phen)$_2$]$^{+/2+}$	**N719**	0.57	0.48	0.43	-	0.12	[119]
[Cu(bpy-(COOEt)$_2$)$_2$]$^+$		-	-	0.57	35	-	
[Cu(bpy-(COOnbut)$_2$)$_2$]$^+$	**Z907**	-	-	-	20	-	[122]
[Cu(bpy-(COOTbut)$_2$)$_2$]$^+$		-	-	-	-	-	
[Cu(PQ)$_2$]$^+$	**Z907**	-	-	-	30	-	[122]
[Cu(MeTbPQ)$_2$]$^+$	**Z907**		-	0.63	35	-	[122]
[Cu(BQ)$_2$]$^+$	**Z907**	-	-	-	-	-	[122]
[Cu(dmp)$_2$]$^{2+/+}$	**C218**	0.93	11.29	-	0.66	-	[121]
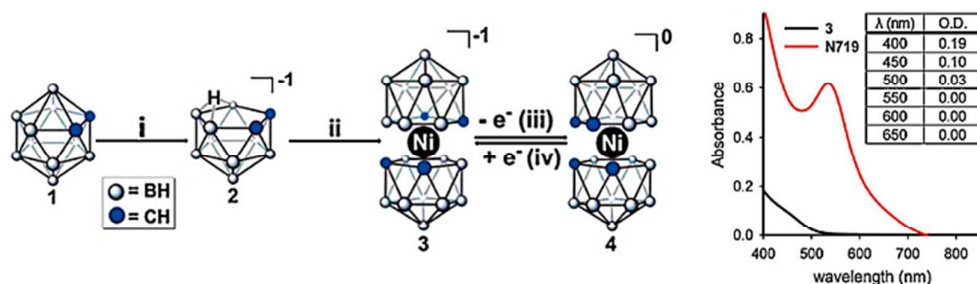
Fig. 14 Ni(III/IV)bis(dicarbollide) complexes and optical absorption spectrum of the shuttles compared to that of N719. Reproduced with permission from ref. 31. Copyright 2010, American Chemical Society.

Additionally, the redox potentials of Ni complexes were systematically tuned through chemical functionalization of Ni(III/IV)bis(dicarbollide) complex in the B(9/12) positions with different electron-donating and electron-withdrawing groups.[124]The presence of electron withdrawn groups makes the redox potential more positive leading to higher V_{oc}. Using Ni(III/IV) shuttles, device power conversion efficiencies achieved in the range of 0.7% to 2.0%.

However, utilization of high-area photoanodes consisting silica aerogels, overcoated by atomic-layer-deposited TiO_2 in DSSCs with a Ni(III/IV)bis(dicarbollide) redox shuttle results in a more than 2-fold enhancement in photocurrent densities, in comparison to similar cells containing photoanodes constructed from TiO_2 nanoparticles.[125] This effect is attributed to a combination of improved electron transport, enhanced recombination resistance across the TiO_2/mediator interface, and the higher light scattering within the aerogel films. Consequently, DSSC charge collection efficiencies with this comparatively fast exchanging outer-sphere redox shuttle are improved in the TiO_2 aerogel templated photoanode. Applying the transmission line model to DSSCs utilizing the Ni(III)/(IV)bis(dicarbollide) redox shuttle, the overall recombination resistance R_{rec} was determined to be $\sim 10^2$ smaller for Ni(IV)bis(dicarbollide) than for I_3^- (Fig. 15). As shown in Fig. 15b effective diffusion length L_n obtained in the presence of Ni(III)/(IV)bis(dicarbollide) is approximately half the ratio achieved in the presence of I^-/I_3^-, at potentials near their respective V_{oc} values.

One of the important advantages of using transition metal complexes as redox shuttles in DSSCs is that their redox potentials can be tuned by modifying the ligands, as distinguished from the I^-/I_3^- system. In 2013, the oxidovanadium(IV/V) couple ($[VO(salen)]^{0/+}$) introduced as a mediator in DSSCs.[30] The redox potential of the $[VO(salen)]^{0/+}$ couple was desirable for the mediator to increase the photovoltage as it is ca. 0.3 V more positive than that

of the conventional I^-/I_3^- couple at 0.34 V vs. Ag/AgCl, as well as the suitability for regenerating or reducing the oxidized dye molecules. Due to more positive potential of $[VO(salen)]^{0/+}$ rather than that of the iodide, it attained a larger V_{oc}. A photoconversion efficiency of η= 5.4% attained with a cell composed of the 2.1 μm thickness TiO_2 layer co-adsorbed with D205/D131[126] in conjugation with $[VO(salen)]^{0/+}$ redox couple.[30] The heterogeneous electron transfer rate constant k_o value for $[VO(salen)]^{0/+}$ was much larger than that of the iodide couple (5.3×10^{-3} cm s^{-1}). A more important factor dominating the mediation process, the bimolecular exchange rate k_{ex} for $[VO(salen)]^{0/+}$, was even larger than those of $Fc^{0/+}$ in the order of 10^6 M^{-1} s^{-1} and was close to the very rapid reaction reported for $[Co(bpy)_3]^{2+/3+}$ (10^{10} M^{-1} s^{-1}).

Apostolopoulou reported the syntheses and physicochemical characterization of the square pyramidal oxidovanadium(IV/V) complexes $(Ph_4P)_2[V^{IV}O(hybeb)]$ and $Ph_4P[V^VO(hybeb)]$, where hybeb^{4-} is a tetradentatediamidodiphenolate(4-) ligand, as new redox mediators in DSSCs.[127] The ideal properties of the complexes, comprising the large electron exchange and transfer rates and the reversible redox process resulting from EPR and electrochemistry, render the vanadium complexes suitable as candidates for redox shuttles in DSSCs. With comparison the oxidovanadium(IV/V) complexes $[VO(hybeb)]^{2-/-}$, $[VO(salen)]^{0/+}$, and I^-/I_3^--based electrolytes, it is found that the main difference between them is the $E_{1/2}$ of the redox couple $[VO(hybeb)]^{2-/-}$, which is 0.49 and 0.63 V less positive than redox potential of $[VO(salen)]^{0/+}$ and I^-/I_3^- respectively. The highest energy conversion efficiency of 2% obtained with the commercial Ru-based sensitizer N719 absorbed on a TiO_2 semiconducting film, in the DSSC under simulated sunlight. However, the theoretical studies discovered that the HOMO of $[VO(hybeb)]^{2-}$ is more positive than the HOMO of the N719 dye, but this energy difference is fairly small; thus, the driving force for dye regeneration should not be optimal.[127]
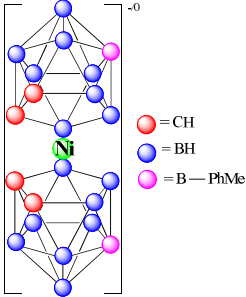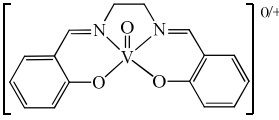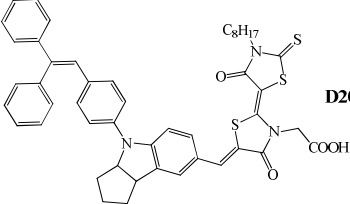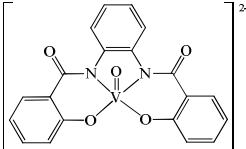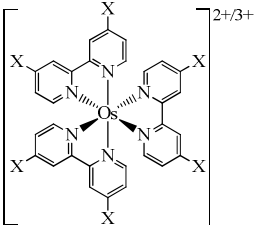
Hamann et al. studied self-exchange and interfacial electron transfer rate constants in two different osmium redox systems including $[Os(dtb)_3]^{2+/3+}$ and $[Os(dmb)_3]^{2+/3+}$.[128] Their results indicated that by attaching the bulky tert-butyl to the bipyridyl ligand, both self-exchange and interfacial electron transfer reactions becomes slower than un-substituted bpy by 50 and 100 times, respectively. This could be mainly because the tert-butyl group can act as a spacer on an outer-sphere redox couple and meaningfully decrease the electronic coupling of the electron transfer reaction in both self-exchange and interfacial electron-transfer processes.

The structures of various alternate redox couples based on Ni, V and Os used in DSSC and also the composition of electrolytes and photovoltaic parameters are tabulated in Table 6.
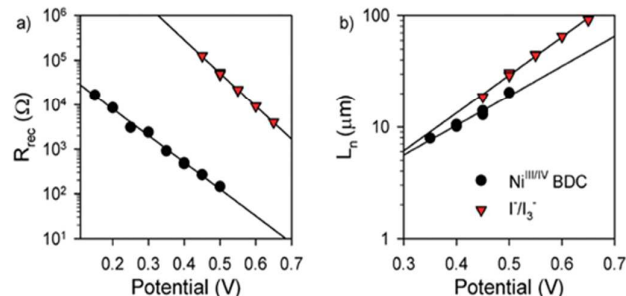
Fig. 15 Potential dependence of (a) charge recombination resistance R_{rec} and (b) diffusion length L_n for Ni(III/IV)bis(dicarbollide) and I^-/I_3^- DSSCs. Reproduced with permission from ref. 125. Copyright 2011, American Chemical Society.

Table 6 Photovoltaic parameters for DSSCs based on mediators of Ni, V and Os in combination with different dyes.

Electrolyte	Sensitizer	V_{oc} (V)	I_{sc} (mA cm^{-2})	FF	IPCE (%)	η (%)	Ref.
[Ni(PhMe-carbollide)$_2$]$^{-/0}$ (= CH, = BH, = B—PhMe)	N719	-	-	-	-	2.0	[124]
[VO(salen)]$^{0/+}$	D205/D131	0.74	12.3	0.59	-	5.4	[30]
[VO(hybeb)]$^{2-/-}$	N719	0.66	5.2	0.58	-	2	[127]
X= metthyl [Os(dmb)$_3$]$^{2+/3+}$ X= tert-butyl [Os(dtb)$_3$]$^{2+/3+}$	-	-	-	-	-	-	[128]

6. Conclusion

In recent five years, significant advances have been realized in the modification and application of iodine free electrolyte-based DSSCs. Since Feldt and co-workers reported their revolutionary work in 2010 regarding to the power conversion efficiency of 6.8% based on organic dye with Co(II/III) complex mediator, an increasing number of laboratories focused on new transition metal complex electrolytes alternative to the I^-/I_3^-. The first results obtained by Gratzel and co-workers in 2011. They found that by adding Co polypyridyl shuttle mediator to new porphyrin sensitizer, they were able to improve the conversion efficiency over 12%. In 2014, the second breakthrough was achieved by coupling another push-pull porphyrin dye with a redox shuttle based on Co bipyridyl derivates. It allowed to a single device the efficiency record of 13%. Therefore, the design and development of the alternative redox electrolytes to traditional I^-/I_3^- are crucial and preferred for the future DSSCs progresses.

The efforts in introducing novel transition metal complex mediators led to a deeper understanding of the dye regeneration processes and also improved the control of the open circuit voltage. The control improvement was originated via the optimization of accepting electrons from the reduced state of the redox couple and produced the oxidized state of the redox couple in electrolyte. Moreover, the key issue for the improvement of photovoltaic properties of DSSCs is developing the suitable photosensitizer to match the different redox couples. It is worth noting that one of the major advantages of using transition metal complexes as redox couples in DSSCs is that their redox potentials can be tuned by modifying the ligands. As distinguished from the I^-/I_3^- system, the redox couple medium must be in balance with the charge transporting ability as well as match with the HOMO energy level of the dye. These could be another interesting and attractive research topic in this field.

As a consequence, this review decides to show the important progress achieved in the mediator research area of DSSCs and analyze the advantages as well as the disadvantages of these complex redox couples to speed up further development of transition metal complex electrolytes.

Acknowledgements

Babak Pashaei (right) is a Ph.D. student (2014-present) in Inorganic Chemistry at the University of Zanjan as a member of the Prof. Shahroosvand group. He obtained his M.Sc. degree at the Institute for Advanced Studies in Basic Sciences (IASBS) with a thesis on "Manganese Oxides as Models for Water Oxidizing Complex in Photosystem II" under the supervision of Prof. Mohammad Mahdi Najafpour. He started his Ph.D. thesis on the "synthesis of ruthenium molecular sensitizers based on phenanthroline derivates for DSSCs".

Hashem Shahroosvand (middle) obtained his M.Sc. degree in Inorgainc chemistry from University of Sistan & baluchestan (2004). He received a Ph.D. in Inorganic Chemistry under supervision of Prof. Mozhgan Khorasani Motlagh. Then he conducted postdoctoral work in group Prof. Nasser Safari and Prof. Ezeddin Mohajerani, University of Shahid Beheshti (2008-2009). He joint to University of Zanjan, where he is currently an Associate Professor in Inorganic Chemistry. His current research interests are in the design and synthesis of nanomaterials for optoelectronic applications and design functionalized polypyridyl complexes for OLEDs and DSSCs applications.

Parisa Abbasi (left) obtained her MSc degree entitled "Synthesis and characterization of novel complexes sensitized solar cell based on the precursors of phendione and non-carboxylic acid" at University of Zanjan, Zanjan, Iran, under supervision of Prof. Hashem Shahroosvand. She joined to Prof. Melanie Pilkington's group in Brock University, ON, Canada (2015-Now). Her PhD Studies will be on "Dual property MRI contrast agents for medical diagnostics".

Notes and references

1. X. Zhang, J. Mao, D. Wang, X. Li, J. Yang, Z. Shen, W. Wu, J. Li, H. Ågren and J. Hua, *ACS Appl. Mater. Interfaces*, 2015, **7**, 2760-2771.

2. J. Gong, J. Liang and K. Sumathy, *Renew. Sust. Energ. Rev.*, 2012, **16**, 5848-5860.

3. K. Hara, H. Horiuchi, R. Katoh, L. P. Singh, H. Sugihara, K. Sayama, S. Murata, M. Tachiya and H. Arakawa, *J. Phys. Chem. B*, 2002, **106**, 374-379.

4. R. Katoh, A. Furube, T. Yoshihara, K. Hara, G. Fujihashi, S. Takano, S. Murata, H. Arakawa and M. Tachiya, *J. Phys. Chem. B*, 2004, **108**, 4818-4822.

5. H. Shahroosvand, S. Rezaei and S. Abbaspour, *J. Photochem. Photobiol., B*, 2014.

6. Z. Yu, N. Vlachopoulos, M. Gorlov and L. Kloo, *Dalton Trans.*, 2011, **40**, 10289-10303.

7. M. Wang, C. Grätzel, S. M. Zakeeruddin and M. Grätzel, *Energy Environ. Sci.*, 2012, **5**, 9394-9405.

8. T. Daeneke, T.-H. Kwon, A. B. Holmes, N. W. Duffy, U. Bach and L. Spiccia, *Nat. Chem.*, 2011, **3**, 211-215.

9. K. B. Aribia, T. Moehl, S. M. Zakeeruddin and M. Grätzel, *Chem. Sci.*, 2013, **4**, 454-459.

10. H. Nishide and T. Suga, *Electrochem. Soc. Interface*, 2005, **14**, 32-36.

11. Z. Zhang, P. Chen, T. N. Murakami, S. M. Zakeeruddin and M. Grätzel, *Adv. Funct. Mater.*, 2008, **18**, 341-346.

12. M. Wang, N. Chamberland, L. Breau, J.-E. Moser, R. Humphry-Baker, B. Marsan, S. M. Zakeeruddin and M. Grätzel, *Nat. Chem.*, 2010, **2**, 385-389.

13. F. Kato, N. Hayashi, T. Murakami, C. Okumura, K. Oyaizu and H. Nishide, *Chem. Lett.*, 2010, **39**, 464-465.

14. D. Li, H. Li, Y. Luo, K. Li, Q. Meng, M. Armand and L. Chen, *Adv. Funct. Mater.*, 2010, **20**, 3358-3365.

15. H. Tian, X. Jiang, Z. Yu, L. Kloo, A. Hagfeldt and L. Sun, *Angew. Chem. Int. Ed.*, 2010, **49**, 7328-7331.

16. H. Tian, E. Gabrielsson, Z. Yu, A. Hagfeldt, L. Kloo and L. Sun, *Chem. Commun.*, 2011, **47**, 10124-10126.

17. U. Bach, D. Lupo, P. Comte, J. Moser, F. Weissörtel, J. Salbeck, H. Spreitzer and M. Grätzel, *Nature*, 1998, **395**, 583-585.

18. G. Larramona, C. Choné, A. Jacob, D. Sakakura, B. Delatouche, D. Péré, X. Cieren, M. Nagino and R. Bayón, *Chem. Mater.*, 2006, **18**, 1688-1696.

19. J. Xia, N. Masaki, M. Lira-Cantu, Y. Kim, K. Jiang and S. Yanagida, *J. Am. Chem. Soc.*, 2008, **130**, 1258-1263.

20. S. Yanagida, Y. Yu and K. Manseki, *Acc. Chem. Res.*, 2009, **42**, 1827-1838.

21. X. Liu, W. Zhang, S. Uchida, L. Cai, B. Liu and S. Ramakrishna, *Adv. Mater.*, 2010, **22**, E150-E155.

22. S. Ahmad, J.-H. Yum, Z. Xianxi, M. Grätzel, H.-J. Butt and M. K. Nazeeruddin, *J. Mater. Chem.*, 2010, **20**, 1654-1658.

23. K. Manseki, W. Jarernboon, Y. Youhai, K.-J. Jiang, K. Suzuki, N. Masaki, Y. Kim, J. Xia and S. Yanagida, *Chem. Commun.*, 2011, **47**, 3120-3122.

24. J.-H. Yum, E. Baranoff, F. Kessler, T. Moehl, S. Ahmad, T. Bessho, A. Marchioro, E. Ghadiri, J.-E. Moser and C. Yi, *Nat. Commun.*, 2012, **3**, 631.

25. S. M. Feldt, E. A. Gibson, E. Gabrielsson, L. Sun, G. Boschloo and A. Hagfeldt, *J. Am. Chem. Soc.*, 2010, **132**, 16714-16724.

26. Y. Xie and T. W. Hamann, *J. Phys. Chem. Lett.*, 2013, **4**, 328-332.

27. H. N. Tsao, C. Yi, T. Moehl, J. H. Yum, S. M. Zakeeruddin, M. K. Nazeeruddin and M. Grätzel, *ChemSusChem*, 2011, **4**, 591-594.

28. A. Bard, M. Stratmann, A. Bard and M. Stratmann, Wiley-VCH: Weinheim, Germany, 2006, vol. 7, pp. 79-106.

29. M. Vlasiou, C. Drouza, T. A. Kabanos and A. D. Keramidas, *J. Inorg. Biochem.*, 2015.

30. K. Oyaizu, N. Hayo, Y. Sasada, F. Kato and H. Nishide, *Dalton Trans.*, 2013, **42**, 16090-16095.

31. T. C. Li, A. M. Spokoyny, C. She, O. K. Farha, C. A. Mirkin, T. J. Marks and J. T. Hupp, *J. Am. Chem. Soc.*, 2010, **132**, 4580-4582.

32. B. A. Gregg, F. Pichot, S. Ferrere and C. L. Fields, *J. Phys. Chem. B*, 2001, **105**, 1422-1429.

33. S. A. Sapp, C. M. Elliott, C. Contado, S. Caramori and C. A. Bignozzi, *J. Am. Chem. Soc.*, 2002, **124**, 11215-11222.

34. S. Cazzanti, S. Caramori, R. Argazzi, C. M. Elliott and C. A. Bignozzi, *J. Am. Chem. Soc.*, 2006, **128**, 9996-9997.

35. M. J. Scott, J. J. Nelson, S. Caramori, C. A. Bignozzi and C. M. Elliott, *Inorg. Chem.*, 2007, **46**, 10071-10078.

36. A. K. Chandiran, N. Tetreault, R. Humphry-Baker, F. Kessler, E. Baranoff, C. Yi, M. K. Nazeeruddin and M. Grätzel, *Nano Lett.*, 2012, **12**, 3941-3947.

37. J. J. Nelson, T. J. Amick and C. M. Elliott, *J. Phys. Chem. C*, 2008, **112**, 18255-18263.

38. M. Liberatore, L. Burtone, T. Brown, A. Reale, A. Di Carlo, F. Decker, S. Caramori and C. Bignozzi, *Appl. Phys. Lett*, 2009, **94**, 173113.

39. B. M. Klahr and T. W. Hamann, *J. Phys. Chem. C*, 2009, **113**, 14040-14045.

40. M. J. DeVries, M. J. Pellin and J. T. Hupp, *Langmuir*, 2010, **26**, 9082-9087.

41. M. Konstantakou, T. Stergiopoulos, V. Likodimos, G. C. Vougioukalakis, L. Sygellou, A. G. Kontos, A. Tserepi and P. Falaras, *J. Phys. Chem. C*, 2014, **118**, 16760-16775.

42. S. M. Feldt, E. A. Gibson, G. Wang, G. Fabregat, G. Boschloo and A. Hagfeldt, *Polyhedron*, 2014, **82**, 154-157.

43. M. Pazoki, N. Taghavinia, A. Hagfeldt and G. Boschloo, *J. Phys. Chem. C*, 2014, **118**, 16472-16478.

44. N. Cai, R. Li, Y. Wang, M. Zhang and P. Wang, *Energy Environ. Sci.*, 2013, **6**, 139-147.

45. P. Gao, Y. J. Kim, J.-H. Yum, T. W. Holcombe, M. K. Nazeeruddin and M. Grätzel, *J. Mater. Chem. A*, 2013, **1**, 5535-5544.

46. T. M. Koh, K. Nonomura, N. Mathews, A. Hagfeldt, M. Grätzel, S. G. Mhaisalkar and A. C. Grimsdale, *J. Phys. Chem. C*, 2013, **117**, 15515-15522.

47. H. Tian and L. Sun, *J. Mater. Chem.*, 2011, **21**, 10592-10601.

48. D. Martineau, M. Beley, P. C. Gros, S. Cazzanti, S. Caramori and C. A. Bignozzi, *Inorg. Chem.*, 2007, **46**, 2272-2277.

49. A. Grabulosa, M. Beley, P. C. Gros, S. Cazzanti, S. Caramori and C. A. Bignozzi, *Inorg. Chem.*, 2009, **48**, 8030-8036.

50. S. Caramori, J. Husson, M. Beley, C. A. Bignozzi, R. Argazzi and P. C. Gros, *Chem. Eur. J.*, 2010, **16**, 2611-2618.

51. Y. Liu, J. R. Jennings, Y. Huang, Q. Wang, S. M. Zakeeruddin and M. Grätzel, *J. Phys. Chem. C*, 2011, **115**, 18847-18855.

52. S. Amit Kumar, M. Urbani, M. Medel, M. Ince, D. Gonzalez-Rodriguez, A. K. Chandiran, A. N. Bhaskarwar, T. s. Torres, M. K. Nazeeruddin and M. Grätzel, *J. Phys. Chem. Lett.*, 2014, **5**, 501-505.

RSC Advances Accepted Manuscript

ARTICLE

53. A. Yella, H.-W. Lee, H. N. Tsao, C. Yi, A. K. Chandiran, M. K. Nazeeruddin, E. W.-G. Diau, C.-Y. Yeh, S. M. Zakeeruddin and M. Grätzel, *science*, 2011, **334**, 629-634.

54. H.-S. Kim, S.-B. Ko, I.-H. Jang and N.-G. Park, *Chem. Commun.*, 2011, **47**, 12637-12639.

55. J.-Y. Kim, K. J. Lee, S. H. Kang, J. Shin and Y.-E. Sung, *J. Phys. Chem. C*, 2011, **115**, 19979-19985.

56. H. N. Tsao, J. Burschka, C. Yi, F. Kessler, M. K. Nazeeruddin and M. Grätzel, *Energy Environ. Sci.*, 2011, **4**, 4921-4924.

57. S. Carli, E. Busatto, S. Caramori, R. Boaretto, R. Argazzi, C. J. Timpson and C. A. Bignozzi, *J. Phys. Chem. C*, 2013, **117**, 5142-5153.

58. J. He, J. M. Pringle and Y.-B. Cheng, *J. Phys. Chem. C*, 2014, **118**, 16818-16824.

59. J. W. Ondersma and T. W. Hamann, *J. Am. Chem. Soc.*, 2011, **133**, 8264-8271.

60. J. W. Ondersma and T. W. Hamann, *Langmuir*, 2011, **27**, 13361-13366.

61. E. Mosconi, J.-H. Yum, F. Kessler, C. J. Gómez García, C. Zuccaccia, A. Cinti, M. K. Nazeeruddin, M. Grätzel and F. De Angelis, *J. Am. Chem. Soc.*, 2012, **134**, 19438-19453.

62. C. Qin, W. Peng, K. Zhang, A. Islam and L. Han, *Org. Lett.*, 2012, **14**, 2532-2535.

63. L. N. Ashbrook and C. M. Elliott, *J. Phys. Chem. C*, 2013, **117**, 3853-3864.

64. M. J. Marchena, G. de Miguel, B. Cohen, J. A. Organero, S. Pandey, S. Hayase and A. Douhal, *J. Phys. Chem. C*, 2013, **117**, 11906-11919.

65. K. C. Robson, K. Hu, G. J. Meyer and C. P. Berlinguette, *J. Am. Chem. Soc.*, 2013, **135**, 1961-1971.

66. D. Xu, H. Zhang, X. Chen and F. Yan, *J. Mater. Chem. A*, 2013, **1**, 11933-11941.

67. T. N. Murakami, N. Koumura, T. Uchiyama, Y. Uemura, K. Obuchi, N. Masaki, M. Kimura and S. Mori, *J. Mater. Chem. A*, 2013, **1**, 792-798.

68. S. Soman, Y. Xie and T. W. Hamann, *Polyhedron*, 2014, **82**, 139-147.

69. T. N. Murakami, N. Koumura, M. Kimura and S. Mori, *Langmuir*, 2014, **30**, 2274-2279.

70. D. Barpuzary, A. S. Patra, J. V. Vaghasiya, B. G. Solanki, S. S. Soni and M. Qureshi, *ACS Appl. Mater. Interfaces*, 2014, **6**, 12629-12639.

71. J. Lu, B. Zhang, H. Yuan, X. Xu, K. Cao, J. Cui, S. Liu, Y. Shen, Y. Cheng and J. Xu, *J. Phys. Chem. C*, 2014, **118**, 14739-14748.

72. S. Mathew, A. Yella, P. Gao, R. Humphry-Baker, B. F. Curchod, N. Ashari-Astani, I. Tavernelli, U. Rothlisberger, M. K. Nazeeruddin and M. Grätzel, *Nat. Chem.*, 2014, **6**, 242-247.

73. C. Yi, F. Giordano, N. L. Cevey-Ha, H. N. Tsao, S. M. Zakeeruddin and M. Grätzel, *ChemSusChem*, 2014, **7**, 1107-1113.

74. J. Cong, Y. Hao, G. Boschloo and L. Kloo, *ChemSusChem*, 2015, **8**, 264-268.

75. J. Yang, P. Ganesan, J. l. Teuscher, T. Moehl, Y. J. Kim, C. Yi, P. Comte, K. Pei, T. W. Holcombe and M. K. Nazeeruddin, *J. Am. Chem. Soc.*, 2014, **136**, 5722-5730.

76. J. Massin, L. Ducasse, M. Abbas, L. Hirsch, T. Toupance and C. Olivier, *Dyes Pigm.*, 2015, **118**, 76-87.

77. K. Lim, K. Song, Y. Kang and J. Ko, *Dyes Pigm.*, 2015, **119**, 41-48.

78. B. E. Hardin, H. J. Snaith and M. D. McGehee, *Nat. Photonics*, 2012, **6**, 162-169.

79. M. Z. Molla, S. S. Pandey, Y. Ogomi, T. Ma and S. Hayase, 2014.

80. P. Salvatori, G. Marotta, A. Cinti, C. Anselmi, E. Mosconi and F. De Angelis, *J. Phys. Chem. C*, 2013, **117**, 3874-3887.

81. K. Miettunen, T. Saukkonen, X. Li, C. Law, Y. K. Sheng, J. Halme, A. Tiihonen, P. R. Barnes, T. Ghaddar and I. Asghar, *J. Electrochem. Soc.*, 2013, **160**, H132-H137.

82. Y. Liu, J. R. Jennings, S. M. Zakeeruddin, M. Grätzel and Q. Wang, *J. Am. Chem. Soc.*, 2013, **135**, 3939-3952.

83. D. Barpuzary, A. Banik, A. N. Panda and M. Qureshi, *J. Phys. Chem. C*, 2015, **119**, 3892-3902.

84. W. Xiang, F. Huang, Y.-B. Cheng, U. Bach and L. Spiccia, *Energy Environ. Sci.*, 2013, **6**, 121-127.

85. T. Daeneke, Y. Uemura, N. W. Duffy, A. J. Mozer, N. Koumura, U. Bach and L. Spiccia, *Adv. Mater.*, 2012, **24**, 1222-1225.

86. D.-S. Yang, C. Kim, M. Y. Song, H.-Y. Park, J. C. Kim, J.-J. Lee, M. J. Ju and J.-S. Yu, *J. Phys. Chem. C*, 2014, **118**, 16694-16702.

87. S. Carli, L. Casarin, S. Caramori, R. Boaretto, E. Busatto, R. Argazzi and C. A. Bignozzi, *Polyhedron*, 2014, **82**, 173-180.

88. M. Kim, H.-G. Yun, L.-W. Jang, D.-W. Jeon, M. G. Kang, J.-H. Yoon, J.-M. Kim, J. H. Park, I.-H. Lee and J. J. Kim, *J. Power Sources*, 2015, **278**, 32-37.

89. J. Liu, J. Zhang, M. Xu, D. Zhou, X. Jing and P. Wang, *Energy Environ. Sci.*, 2011, **4**, 3021-3029.

90. M. Zhang, J. Liu, Y. Wang, D. Zhou and P. Wang, *Chem. Sci.*, 2011, **2**, 1401-1406.

91. M. Xu, D. Zhou, N. Cai, J. Liu, R. Li and P. Wang, *Energy Environ. Sci.*, 2011, **4**, 4735-4742.

92. Y. Bai, J. Zhang, D. Zhou, Y. Wang, M. Zhang and P. Wang, *J. Am. Chem. Soc.*, 2011, **133**, 11442-11445.

93. X. Zong, M. Liang, C. Fan, K. Tang, G. Li, Z. Sun and S. Xue, *J. Phys. Chem. C*, 2012, **116**, 11241-11250.

94. X. Zong, M. Liang, T. Chen, J. Jia, L. Wang, Z. Sun and S. Xue, *Chem. Commun.*, 2012, **48**, 6645-6647.

95. Z. Wang, M. Liang, L. Wang, Y. Hao, C. Wang, Z. Sun and S. Xue, *Chem. Commun.*, 2013, **49**, 5748-5750.

96. K. Kakiage, Y. Aoyama, T. Yano, T. Otsuka, T. Kyomen, M. Unno and M. Hanaya, *Chem. Commun.*, 2014, **50**, 6379-6381.

97. S. Koussi-Daoud, D. Schaming, L. Fillaud, G. Trippé-Allard, F. Lafolet, E. Polanski, K. Nonomura, N. Vlachopoulos, A. Hagfeldt and J.-C. Lacroix, *Electrochim. Acta*, 2015.

98. W. Gao, M. Liang, Y. Tan, M. Wang, Z. Sun and S. Xue, *J. Power Sources*, 2015, **283**, 260-269.

99. Y. Zhang, Z.-h. Wang, Y.-j. Hao, Q.-p. Wu, M. Liang and S. Xue, *Chin. J. Chem. Phys.*, 2015, **28**, 91-100.

100. D. Zhou, Q. Yu, N. Cai, Y. Bai, Y. Wang and P. Wang, *Energy Environ. Sci.*, 2011, **4**, 2030-2034.

101. H. Nusbaumer, J.-E. Moser, S. M. Zakeeruddin, M. K. Nazeeruddin and M. Grätzel, *J. Phys. Chem. B*, 2001, **105**, 10461-10464.

102. H. Nusbaumer, S. M. Zakeeruddin, J. E. Moser and M. Grätzel, *Chem. Eur. J.*, 2003, **9**, 3756-3763.

103. P. J. Cameron, L. M. Peter, S. M. Zakeeruddin and M. Grätzel, *Coord. Chem. Rev.*, 2004, **248**, 1447-1453.

104. H. Wang, P. G. Nicholson, L. Peter, S. M. Zakeeruddin and M. Grätzel, *J. Phys. Chem. C*, 2010, **114**, 14300-14306.

105. L. Kavan, J.-H. Yum, M. K. Nazeeruddin and M. Grätzel, *ACS Nano*, 2011, **5**, 9171-9178.

106. J.-H. Yum, T. Moehl, J. Yoon, A. K. Chandiran, F. Kessler, P. Gratia and M. Grätzel, *J. Phys. Chem. C*, 2014, **118**, 16799-16805.

107. S. Ahmad, T. Bessho, F. Kessler, E. Baranoff, J. Frey, C. Yi, M. Grätzel and M. K. Nazeeruddin, *Phys. Chem. Chem. Phys.*, 2012, **14**, 10631-10639.

108. M. K. Kashif, J. C. Axelson, N. W. Duffy, C. M. Forsyth, C. J. Chang, J. R. Long, L. Spiccia and U. Bach, *J. Am. Chem. Soc.*, 2012, **134**, 16646-16653.

109. M. K. Kashif, M. Nippe, N. Duffy, C. M. Forsyth, C. J. Chang, J. R. Long, L. Spiccia and U. Bach, *Angew. Chem.*, 2013, **125**, 5637-5641.

110. P. K. Palomaki, M. R. Civic and P. H. Dinolfo, *ACS Appl. Mater. Interfaces*, 2013, **5**, 7604-7612.

111. S. Powar, T. Daeneke, M. T. Ma, D. Fu, N. W. Duffy, G. Götz, M. Weidelener, A. Mishra, P. Bäuerle and L. Spiccia, *Angew. Chem.*, 2013, **125**, 630-633.

112. S. M. Feldt, U. B. Cappel, E. M. Johansson, G. Boschloo and A. Hagfeldt, *J. Phys. Chem. C*, 2010, **114**, 10551-10558.

113. T. W. Hamann, O. K. Farha and J. T. Hupp, *J. Phys. Chem. C*, 2008, **112**, 19756-19764.

114. S. M. Waita, B. O. Aduda, J. M. Mwabora, G. A. Niklasson, C. G. Granqvist and G. Boschloo, *J. Electroanal. Chem.*, 2009, **637**, 79-83.

115. T. Daeneke, A. J. Mozer, T.-H. Kwon, N. W. Duffy, A. B. Holmes, U. Bach and L. Spiccia, *Energy Environ. Sci.*, 2012, **5**, 7090-7099.

116. Y. Tachibana, K. Umekita, Y. Otsuka and S. Kuwabata, *J. Phys. D: Appl. Phys.*, 2008, **41**, 102002.

117. I. A. Rutkowska, A. Andrearczyk, S. Zoladek, M. Goral, K. Darowicki and P. J. Kulesza, *J. Solid State Electrochem.*, 2011, **15**, 2545-2552.

118. I. R. Perera, T. Daeneke, S. Makuta, Z. Yu, Y. Tachibana, A. Mishra, P. Bäuerle, C. A. Ohlin, U. Bach and L. Spiccia, *Angew. Chem. Int. Ed.*, 2015, **54**, 3758-3762.

119. S. Hattori, Y. Wada, S. Yanagida and S. Fukuzumi, *J. Am. Chem. Soc.*, 2005, **127**, 9648-9654.

120. S. Ardo and G. J. Meyer, *Chem. Soc. Rev.*, 2009, **38**, 115-164.

121. Y. Bai, Q. Yu, N. Cai, Y. Wang, M. Zhang and P. Wang, *Chem. Commun.*, 2011, **47**, 4376-4378.

122. M. Brugnati, S. Caramori, S. Cazzanti, L. Marchini, R. Argazzi and C. A. Bignozzi, *Int. J. Photoenergy*, 2008, **2007**.

123. C.-C. Yuan, S.-M. Wang, W.-L. Chen, L. Liu, C. Qin, Z.-M. Su and E.-B. Wang, *Dalton Trans.*, 2014, **43**, 1493-1497.

124. A. M. Spokoyny, T. C. Li, O. K. Farha, C. W. Machan, C. She, C. L. Stern, T. J. Marks, J. T. Hupp and C. A. Mirkin, *Angew. Chem.*, 2010, **122**, 5467-5471.

125. T. C. Li, F. Fabregat-Santiago, O. K. Farha, A. M. Spokoyny, S. R. Raga, J. Bisquert, C. A. Mirkin, T. J. Marks and J. T. Hupp, *J. Phys. Chem. C*, 2011, **115**, 11257-11264.

126. S. Ito, H. Miura, S. Uchida, M. Takata, K. Sumioka, P. Liska, P. Comte, P. Péchy and M. Grätzel, *Chem. Commun.*, 2008, 5194-5196.

127. A. Apostolopoulou, M. Vlasiou, P. A. Tziouris, C. Tsiafoulis, A. C. Tsipis, D. Rehder, T. A. Kabanos, A. D. Keramidas and E. Stathatos, *Inorg. Chem.*, 2015, **54**, 3979-3988.

128. T. W. Hamann, B. S. Brunschwig and N. S. Lewis, *J. Phys. Chem. B*, 2006, **110**, 25514-25520.